



**Carolina Branquinho
de Matos**

**Unravelling the peroxisome-dependent MAVS
signalling pathway**

**Estudo da via de sinalização dependente da MAVS
peroxisomal**



**Carolina Branquinho
de Matos**

**Unravelling the peroxisome-dependent MAVS
signalling pathway**

**Estudo da via de sinalização dependente da MAVS
peroxisomal**

Tese apresentada à Universidade de Aveiro para cumprimento dos requisitos necessários à obtenção do grau de Mestre em Biomedicina Molecular, realizada sob a orientação científica da Dra. Daniela Maria Oliveira Gandra Ribeiro, Investigadora Auxiliar do Departamento de Ciências Médicas e Investigadora Principal do “Virus Host-Cell Interactions Laboratory” do Instituto de Biomedicina (iBiMED), Universidade de Aveiro.

Thesis submitted at University of Aveiro to fulfil the requirements to obtain the Master’s Degree in Molecular Biomedicine, held under the scientific guidance of Dr. Daniela Maria Oliveira Gandra Ribeiro, Assistant Researcher at the Medical Sciences Department of the University of Aveiro and Group leader of the “Virus Host-Cell Interactions Laboratory” at Institute of Biomedicine (iBiMED), University of Aveiro.

This work was supported by the Portuguese Foundation for Science and Technology (FCT): PTDC/BIA-CEL/31378/2017 (POCI-01-0145-FEDER-031378), UID/BIM/04501/2013, POCI-01-0145-FEDER-007628 under the scope of the Operational Program “Competitiveness and internationalization”, in its FEDER/FNR component.

Dedico esta tese aos meus pais.

o júri

presidente

Doutora Ana Margarida Domingos Tavares de Sousa

Professora Auxiliar Convidada do Departamento de Ciências Médicas da Universidade de Aveiro

Doutora Daniela Maria Oliveira Gandra Ribeiro

Investigadora Auxiliar do Departamento de Ciências Médicas da Universidade de Aveiro

Doutora Ana Sofia da Cunha Guimarães

Investigadora de Pós-doutoramento do Instituto de Investigação e Inovação em Saúde da Universidade do Porto

agradecimentos

Mais uma etapa que está a chegar ao fim e, como não podia deixar de ser, quero agradecer a todas as pessoas que me ajudaram e acompanharam neste percurso.

À Dra. Daniela Ribeiro, por me ter acolhido tão bem no seu grupo, pela orientação ao longo do projeto, por partilhar comigo todo o seu conhecimento e entusiasmo pela área da ciência e da virologia. Obrigada por ter acreditado em mim.

Aos meus ex-colegas e colegas de trabalho, que me integraram logo no grupo e tornaram toda esta experiência uma das melhores que já tive.

Ao Bruno e ao Alexandre, pela companhia e apoio nesta aventura.

À Rita, pela ajuda que sempre me deste, por me incentivares a ser melhor, por me ensinares e dares os truques precisos para ser uma ótima cientista e me obrigares a responder às minhas próprias perguntas porque sempre acreditaste nas minhas capacidades. És uma inspiração.

À Mariana, por todos os momentos maravilhosos que passámos dentro e fora do laboratório. Obrigada por aturares as minhas cantorias, pelo apoio, por não teres desistido de mim e acreditares que conseguia. Obrigada pelas gargalhadas, pelo conhecimento, por toda a tua amizade. És incrível, obrigada por tudo.

À Marisa, por estares sempre disponível para ajudar, por acreditares em mim e por festejares as minhas conquistas comigo.

Às amigas maravilhosas que conheci aqui neste mestrado, sem vocês não teria metade da graça. Obrigada pelos jantares, pelas gargalhadas, por me incentivarem a lutar pelo que queria. Um agradecimento especial à Daniela e à Inês, que me ouviram quando estava a ter crises existenciais e acalmaram quando mais precisei (vocês aturaram-me muito!).

Aos meus amigos Lisboaetas, que apesar de eu os ter “abandonado” não desistiram de mim e apoiaram sempre as minhas decisões. Um obrigada enorme às minhas amigas de longa data, Rita e Catarina, que apesar de não perceberem nada do que faço, sempre me motivaram a ir mais longe, a lutar pelos meus sonhos e animaram nos momentos mais difíceis. Vocês são as melhores.

À Catarina, que mesmo estando a quilómetros de distância perdia sempre umas horinhas para fazermos videochamadas, ouvir os meus problemas e ajudar-me a ultrapassá-los. Sem ti a minha sanidade mental já tinha desaparecido.

Por último, um obrigada do tamanho do mundo à minha família, pelo apoio gigante que sempre me deram, por acreditarem nas minhas decisões, por me tornarem numa pessoa melhor e incentivarem a lutar por aquilo que quero. Obrigada por estarem sempre presentes mesmo estando longe e por se mostrarem interessados no meu trabalho, mesmo não “pescando” nada do assunto. Sem vocês nada seria possível.

palavras-chave

Peroxisomas, vírus, MAVS, sinalização antiviral

resumo

A resposta imunitária antiviral celular é desencadeada após o reconhecimento de componentes virais específicos por um conjunto de proteínas hospedeiras, como é o caso do gene Indutível pelo ácido retinóico I (RIG-I). Após estimulação viral, o RIG-I sofre uma mudança conformacional e interage com o adaptador da sinalização antiviral mitocondrial (MAVS) na mitocôndria e peroxisomas, iniciando uma cascata de sinalização que culmina com a produção de efetores antivirais, prevenindo passos importantes na propagação viral.

Já foi demonstrado que os peroxisomas e as mitocôndrias atuam em conjunto como plataformas de sinalização importantes dentro deste mecanismo: enquanto a via peroxisomal induz a rápida expressão de fatores defensivos, providenciando uma proteção a curto-prazo, a via mitocondrial ativa uma cascata de sinalização com uma cinética mais atrasada que amplifica e estabiliza a resposta antiviral. Isto sugere a existência de duas cascatas de sinalização distintas que iniciam em ambos os organelos.

A via de sinalização mitocondrial tem sido extensivamente estudada e a maioria dos seus componentes já foi identificada. Com este estudo, pretendemos desvendar os componentes da via dependente dos peroxisomas, investigando o possível envolvimento de proteínas que também pertencem à via mitocondrial. Para tal, utilizámos células que contêm MAVS unicamente nos peroxisomas e sobreexpressámos proteínas virais que já foram anteriormente demonstradas ser responsáveis pela inibição de passos específicos da via MAVS mitocondrial: UL36 do vírus do herpes simples (que cliva as cadeias de poliubiquitina da TRAF3 inibindo o recrutamento da TBK1) ou NP do vírus da coriomeningite linfocítica (que se associa ao IKK ϵ bloqueando a sua capacidade de fosforilar o IRF3). Estas células foram estimuladas e a sinalização antiviral foi analisada por RT-qPCR e imunodeteção. Os nossos resultados revelaram que a UL36 e a NP também inibem a sinalização antiviral nestas células, indicando desta forma a presença da TRAF3 e IKK ϵ como moléculas “*downstream*” da MAVS na via de sinalização antiviral dependente dos peroxisomas.

keywords

Peroxisomes, viruses, MAVS, antiviral signalling

abstract

The cellular antiviral immune response is triggered upon recognition of specific viral components by a set of host proteins such as the retinoic acid inducible gene-I (RIG-I). Upon viral stimulation, RIG-I undergoes a conformational change and interacts with the mitochondrial antiviral signalling adaptor (MAVS) at mitochondria and peroxisomes, initiating a signalling cascade that culminates with the production of antiviral effectors, preventing important steps in viral propagation.

Peroxisomes and mitochondria have been shown to act in concert as important signalling platforms within this mechanism: while the peroxisomal pathway induces the rapid expression of defense factors providing short-term protection, the mitochondrial pathway activates a signalling cascade with delayed kinetics that amplifies and stabilizes the antiviral response. This suggests the existence of two distinct signalling cascades originating from both organelles.

The mitochondrial signalling pathway has been extensively studied and most of its components have already been identified. With this study, we aimed to unveil the components of the peroxisome-dependent pathway, by investigating the possible involvement of proteins that also belong to the mitochondrial pathway. To that end, we used cells that contain MAVS solely at peroxisomes and overexpressed viral proteins that have been shown to inhibit specific steps of the mitochondrial MAVS pathway: UL36 from herpes simplex virus (shown to cleave the polyubiquitin chains of TRAF3 inhibiting the recruitment of TBK1) or NP from lymphocytic choriomeningitis virus (associates with IKK ϵ blocking its ability to phosphorylate IRF3). These cells were virally-stimulated and antiviral signalling was analysed by RT-qPCR and immunoblot. Our results revealed that UL36 and NP also inhibited the antiviral signalling in these cells, indicating the presence of TRAF3 and IKK ϵ as downstream molecules of MAVS on the peroxisomal-dependent antiviral signalling pathway.

List of Abbreviations

1-0-alkyl-DHAP	1-0-alkyl-dihydroxyacetone phosphate
1-acyl-DHAP	1-acyl-dihydroxyacetone phosphate
ACAA1	3-ketoacyl-CoA thiolase
AcB	Acyl-coenzyme A-binding domain
ACBD5	Acyl-CoA binding domain protein 5
ACOX	Acyl-CoA oxidase
Acyl-CoA	Long-chain fatty acid-Acyl-CoA
AGPS	Alkyldihydroxyacetonephosphate synthase
AIM2	Absent in melanoma 2
APCs	Antigen-presenting cells
ATP	Adenosine triphosphate
CARDs	Caspase activation and recruitment domains
cGAMP	Cyclic guanosine monophosphate-adenosine monophosphate
cGAS	Cyclic guanosine monophosphate-adenosine monophosphate synthase
CLRs	C-type lectin receptors
CTD	C-terminal domain
DAI	DNA-dependent activator of IFN-regulatory factors
DBP	D-bifunctional protein
DCs	Dendritic cells
DENV	Dengue virus
DHAP	Dihydroxyacetone phosphate
DHCA	Dihydroxycholestanoic acid
DLP	Dynamin-like protein
DNA	Deoxynucleic acids
DRP	Dynamin-Related-Protein
dsDNA	Double-stranded DNA
dsRNA	Double-stranded RNA

ECD	Extracellular domain
ER	Endoplasmic reticulum
ERDppVs	Endoplasmic reticulum pre-peroxisomal vesicles
ERGIC	ER-Golgi intermediate compartment
FA	Fatty-acid
FFAT	Two phenylalanine in an acidic tract
FIS1	Mitochondrial fission factor 1
GNPAT	Glycerone phosphate O-Acyltransferase
GPI	Glycosyl phosphatidyl inositol
GTP	Guanosine Triphosphate
GTPase	Guanin triphosphate enzyme
HCV	Hepatitis C virus
HSV-1	Herpes simplex virus 1
IAV	Influenza A virus
IFI16	IFN- γ -inducible protein 16
IFNs	Interferons
IKK	I κ B kinase
IKK ϵ	I κ B kinase epsilon
IPS-1	IFN- β promoter stimulator-1
IRES	Internal ribosomal entry site
IRFs	Interferons regulatory factors
ISG	Interferon-stimulated genes
KO	Knock-out
LBP	L-bifunctional protein
LCMV	Lymphocytic choriomeningitis virus
LD	Lipid Droplets
LDL	Lipoproteins
LDLR	Low-density lipoprotein receptors
LDs	Lipid droplets

LGP2	Laboratory of genetics and physiology 2
LPMC	Lysosome-peroxisome membrane contact
LRRs	Leucine-rich repeats
LYSO	Lysosome
MAM	Mitochondria associated membranes
MAP	Mitogen-activated protein
MAPKs	Mitogen-activated protein kinases
MAVS	Mitochondrial antiviral signalling
MDA5	Melanoma differentiation-associated gene 5
MDppVs	Mitochondrial derived pre-peroxisomal vesicles
MEFs	Mouse embryonic fibroblasts
MFF	Mitochondrial fission factor
MHC1	Major histocompatibility complex class I
MITO	Mitochondria
mPTS	Membrane peroxisomal targeting signal
mRNAs	Mature RNAs
MSP	Major sperm protein
MyD88	Myeloid differentiation primary response gene 88
NDV	Newcastle disease virus
NEMO	NF-kappa-B essential modulator
NF-κB	Nuclear factor kappa-light-chain enhancer of activated B cells
NLR	Nucleotide oligomerization domain-like receptors
NLRs	Nucleotide-binding oligomerization domain (NOD)-like receptors
PAMPs	Pathogen-associated molecular patterns
PBDs	Peroxisome biogenesis disorders
PEDs	Peroxisomal enzyme deficiencies
pER	Pre-peroxisomal endoplasmic reticulum;
PKR	Protein kinase RNA-activated
PMPs	Peroxisomal membrane proteins

PO	Peroxisome
Pol III	DNA-dependent RNA polymerase III
Poly I:C	Polyinosinic: polycytidylic acid
PPIs	Protein-protein interactions
PPR α	Proliferator-activated receptor α
ppVs	Pre-peroxisomal vesicles
PRRs	Pattern recognition receptors
RCDP	Rhizomelic chondrodysplasia punctata
RdRp	RNA-dependent RNA polymerase
RIG-I	Retinoic acid-inducible gene I
RLRs	RIG-I-like receptors
RNA	Ribonucleic acids
ROS	Reactive oxygen species
SCP	Sterol carrier protein
SE	Sterol esters
ssRNA	Single-stranded RNA
STING	Stimulator of interferon genes
TAG	Triacylglycerols
TBK1	TRAF family member associated NF- κ B activator-binding kinase 1
THCA	Trihydroxycholestanoic acid
TIM	TRAF interacting motifs
TIR	Toll/interleukin-1 receptor
TIRAP	TIR domain-containing adaptor protein
TLRs	Toll-like receptors
TNF	Tumor necrosis factor
TRAF	TNF receptor-associated factor
TRAM	TRIF-related adaptor molecule
TRIF	TIR-domain-containing adapter-inducing interferon- β
TRIM25	Tripartite motif-containing 25

UTR	Untranslated regions
VAP	Vesicle-associated membrane protein-associated protein
VISA	Virus-induced signalling adaptor
VLCFAs	Very long-chain-fatty acids
VLDL	Very low-density lipoproteins
VSV	Vesicular stomatitis virus
WNV	West Nile virus
WT	Wild-type
X-ALD	X-linked adrenoleukodystrophy
ZS	Zellweger syndrome

Index

I.	Introduction	1
1.1	Peroxisomes.....	3
	Peroxisome Biogenesis.....	4
	Growth and division model	4
	De novo model	6
	Peroxisomes Functions.....	8
	Oxygen Metabolism and Reactive Oxygen Species	8
	Ether Lipid Synthesis	9
	Fatty Acid β -Oxidation.....	9
	Peroxisomes and other organelles	10
	Peroxisomes and Mitochondria Interaction	10
	Peroxisomes and ER Interaction	11
	Peroxisomes and Lysosomes Interaction	12
	Peroxisomes and Lipid Droplets Interaction.....	12
1.2	Cellular Antiviral Signalling.....	14
	Toll-like receptors	15
	Cytosolic DNA sensors	17
	RIG-I like receptors	19
II.	Aims	25
III.	Materials and Methods	29
3.1	Materials	31
	Cell lines.....	31
	Cell Culture Solutions	31
	Plasmids	32
	Primers and Oligonucleotides	32
	Transfection Reagents	33
	Markers and Loading Dyes.....	33
	Antibodies	33
	Solutions and Buffers	34
	Databases and Software's	35
	Equipment	36
3.2	Methods.....	37
	Cell culture.....	37
	Cell lines maintenance	37

Cell storage, freezing and thawing	37
Transient Mammalian Transfection Methods	38
Lipofectamine 3000	38
Immunofluorescence	38
RT-qPCR	39
Isolation of RNA	39
cDNA synthesis	39
Real-time Quantitative Polymerase Chain Reaction	40
Protein Extraction and Quantification	41
Lysis protocol	41
Bradford quantification method	41
Western Blot	41
Sodium Dodecyl Sulfate-Polyacrylamide Gel Electrophoresis (SDS-PAGE) and	
Transfer	41
Immunoblotting	42
IV. Results and Discussion	43
4.1 TRAF3 is involved in the peroxisomal MAVS downstream signalling	45
4.2 IKK ϵ is involved in the peroxisomal MAVS downstream signalling transduction..	48
V. Conclusion	53
VI. References	57

List of figures

Figure 1. Growth and division for peroxisome biogenesis	6
Figure 2. De novo model for peroxisome biogenesis	7
Figure 3. Oxygen metabolism and reactive oxygen species	8
Figure 4. Ether lipid synthesis	9
Figure 5. Fatty acid β -oxidation.....	10
Figure 6. Peroxisomes and their interaction with other organelles.....	13
Figure 7. TLRs signalling.	16
Figure 8. cGAS-mediated signalling.	18
Figure 9. RLR signalling	23
Figure 10. Reverse transcription PCR cycle of cDNA synthesis	40
Figure 11. RT-qPCR cycling protocol	40
Figure 12. UL36-YFP overexpression in MEFs MAVS-PEX cells	46
Figure 13. Viral protein UL36-YFP inhibits the peroxisome-dependent innate immunity signalling.	47
Figure 14. IKK ϵ is involved in the downstream signalling from peroxisomal MAVS	49
Figure 15. Mitochondrial and peroxisome MAVS-dependent signalling pathway	52

List of tables

Table 1. List of plasmids.....	32
Table 2. List of PCR primers.....	32
Table 3. List of markers and loading dyes.	33
Table 4. List of primary antibodies.	33
Table 5. List of secondary antibodies.	34
Table 6. List of solutions and buffers.	34

I. Introduction

1.1 | Peroxisomes

Peroxisomes were first described as “microbodies” in 1954 by Johannes Rhodin and were characterized as cytoplasmic bodies with a single membrane and a subtle granular matrix that were present in the convoluted tubule cells of the mouse kidney¹. This morphological designation was progressively replaced by the term “peroxisome” that was introduced in 1966 by De Duve and Baudhuin, who isolated this organelle from rat liver containing numerous H₂O₂-producing oxidases and an H₂O₂-degrading enzyme in their matrix²⁻⁴.

Peroxisomes are commonly defined as ubiquitous single membrane bound organelles that have a fine granular matrix with a greatly variable enzymatic content. They are small organelles, with 0.1 to 0.5 micrometers (μm), with a spherical or, in some cases, elongated shape. Peroxisomes’ morphology and function depend not only on the species and cell type, but also on the environmental or developmental conditions⁵. As multifunctional organelles, peroxisomes are signalling platforms to various metabolic pathways related to ageing, defense against pathogens, maintenance of cellular homeostasis, among others. In order to achieve these functions, peroxisomes interact, cooperate and connect with other organelles such as mitochondria, the smooth endoplasmic reticulum and lipid droplets^{4,6,7}. In the latest years, it is becoming clearer that peroxisomes are fundamental for the vitality and development of the organism, as more and more studies support an important peroxisomal role in numerous physiological processes. Peroxisomal functional disruption has been specifically linked to several pathologies, including aging-related diseases, neurodegenerative disorders, and cancer^{3,8-10}.

| Peroxisome Biogenesis

Peroxisomes do not contain DNA or a protein translation machinery and, for that reason, their matrix and membrane proteins are encoded by nuclear genes^{7,11}. The great majority of peroxisomal proteins are synthesized on free polyribosomes in the cytosol and the peroxisomal matrix proteins are folded and assembled previously to peroxisomal import^{3,11,12}.

In recent years, several proteins have been identified as being involved in peroxisomal biogenesis. These proteins, termed peroxins, are evolutionarily conserved and encoded by *PEX* genes. In fact, most of the human peroxisomal disorders results from defects on these peroxins^{13,14}.

Peroxisome biogenesis is being studied and debated for a long time now, and two models' standout. Both have co-existed for decades and probably they co-operate within the same cells in response to specific environmental signals^{12,15}. The growth and division model postulates that the peroxisomes arise from pre-existing ones which grow to a certain size after acquiring all peroxisomal proteins, both peroxisomal matrix and PMPs, directly from the cytosol. Afterwards, they divide by fission with the aim of forming new peroxisomes that will eventually undergo this cycle again^{12,15,16}. On the other hand, the *de novo* model suggests the fusion of pre-peroxisomal vesicles (ppVs), that contain different PMPs, making it possible to create mature or larger peroxisomes in a heterotypic fashion or with pre-existing peroxisomes, respectively^{7,12,15,17}. Recently, a third model arose combining features of both growth and division and the *de novo* models¹⁸.

| Growth and division model

The biogenesis of the peroxisome through the growth and division model can be divided into three principal stages: (1) peroxisomal membrane biogenesis (import of PMPs), (2) import of peroxisomal matrix proteins and, lastly, (3) peroxisome growth and division. Up to now, 32 *PEX* genes have been identified and, most of them, are required for this process^{19–22}.

Initially, it is necessary the import of PMPs which are synthesized on free polyribosomes in the cytoplasm and post-translationally imported and inserted directly into the peroxisome^{15,21}. The peroxins that are responsible for the elaboration and maintenance of this mechanism are PEX19 and PEX3, that act as a chaperone-like factor and a transporter, and, a shuttling receptor, respectively. In general, PEX19 recognizes and binds to the membrane peroxisomal targeting signal (mPTS) motifs in the PMPs and carries the transport of these proteins to the peroxisomal membrane, where it docks with the transmembrane protein PEX3^{15,19,20}. There are two classes of mPTSs: class 1 mPTSs or PTS1, which are bound and imported by PEX19, and class 2 mPTSs or PTS2, that function independently of PEX19. PEX16, a class 1 PMP, serve as a docking factor between PEX3-PEX19 complexes when PEX3 is forced to traffic to peroxisomes using the class 1 pathway^{16,18–20}.

Subsequently, the import of peroxisomal matrix proteins is mediated by the cytosolic receptors PEX5 and PEX7 which recognize and bind, respectively, to PTS1, which comprises a C-terminal tripeptide (SKL) and PTS2. Afterwards, this complex is targeted to the docking PEX13 and PEX14, where the receptors translocate their cargo across the membrane, into the peroxisome lumen, followed by the dissociation of the receptor-cargo complex and the release of the cargo. The receptors are then recycled and exported from the peroxisome matrix to the cytosol^{11,16,20,22,23}.

During the growth and division, three steps can be described involving peroxisome elongation, constriction, and scission (Figure 1). PEX11 β , a peroxisomal transmembrane protein, is the peroxin responsible for the elongation process, allowing the incorporation of lipids into the peroxisomal membrane, and consequently, provokes a curvature to the membrane, forming a tubular structure (Figure 1)^{15,24,25}. After peroxisomal elongation, PEX11 β recruits the anchoring proteins Mitochondrial Fission Factor (MFF) and Mitochondrial Fission 1 (FIS1) to the peroxisomal membrane, which in turn recruit Dynamin Like Protein/ Dynamin-Related-Protein GTPase 1 (DLP/DRP1). This protein forms a ring-like structure around the membrane and, the hydrolysis of GTP, induced by PEX11 β , leads to conformational changes and constriction of the membrane, that ultimately divides the peroxisome (Figure 1)^{15,24,26,27}. The fission machinery must act in tight coordination with the

membrane elongation factors, in order to facilitate the constriction and division of the peroxisomal membrane^{14–16,21,24,28}.

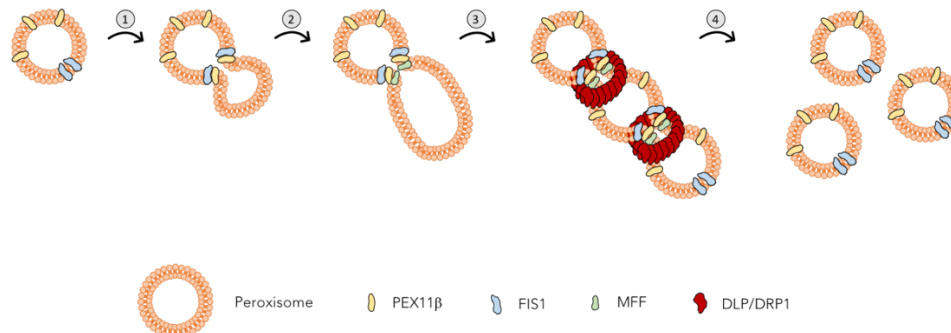


Figure 1. Growth and division for peroxisome biogenesis. This model can be divided into three steps: elongation, constriction, and fission. PEX11 β is activated allowing conformational changes of the peroxisomal membrane in pre-existing peroxisomes forming a tubular structure. MFF and FIS1 are recruited which in turn recruit DLP/DRP1 that will allow the constriction of the membrane and, eventually, to the final fission. (1) and (2) – Elongation; (3) – Constriction; (4) – Fission.

| *De novo model*

The growth and division model was questioned when an explanation for how peroxisomes could be formed in mutant yeast cells with no evidence of pre-existing peroxisomes, due to a mutation in the peroxins PEX3 and PEX19, was not found¹⁵. For that reason, a new model emerged in which some PMPs can be first inserted into the membrane of the ER, sorted to a specific region of the ER, named pER, and finally, pre-peroxisomal vesicles (ppVs) containing this PMPs merge (Figure 2). The *de novo* model can be divided into five main stages: (1) PMP insertion into the ER, (2) intra-ER sorting of PMPs to the pER, (3) PMP exit from the pER in ppVs, (4) ppV fusion with pre-existing peroxisomes and, finally, (5) the potential involvement of ppVs derived from both the ER and mitochondrial membranes (Figure 2)^{15,29}.

For the initiation of the *de novo* peroxisomal biogenesis, is necessary the assembly of the peroxisomal import machinery within a pre-peroxisome. Briefly, this process consists in the import of the PMPs bounded to PEX19 through the receptors PEX3 and PEX16 where they

are inserted into the ER membrane^{11,15–17,30}. Next, after the insertion of the PMPs and their intra-ER sorting into the pER, is necessary to allow the exit of the PMP from the ER where the ppVs are then produced^{30,31}. It is important to note that the ppV production is a highly organized process, which means that while PMPs reside in the ER, PMP import must not occur into the wrong subcellular compartment. Thereunto, PMPs are segregated into distinct ER-derived ppVs (ERDppVs) and, most likely, mitochondrial derived ppVs (MDppVs). There is still some debate on whether or not other organelles like mitochondria are involved in this process. Nevertheless, once ppVs are produced from the ER and possibly from the mitochondria, it is suggested that ERDppVs and MDppVs are capable to fuse forming fully functional peroxisomes (Figure 2)^{11,14,15}. This process needs specific peroxins such as PEX34, PEX16, PEX 3 and PEX 14 in order to happen.

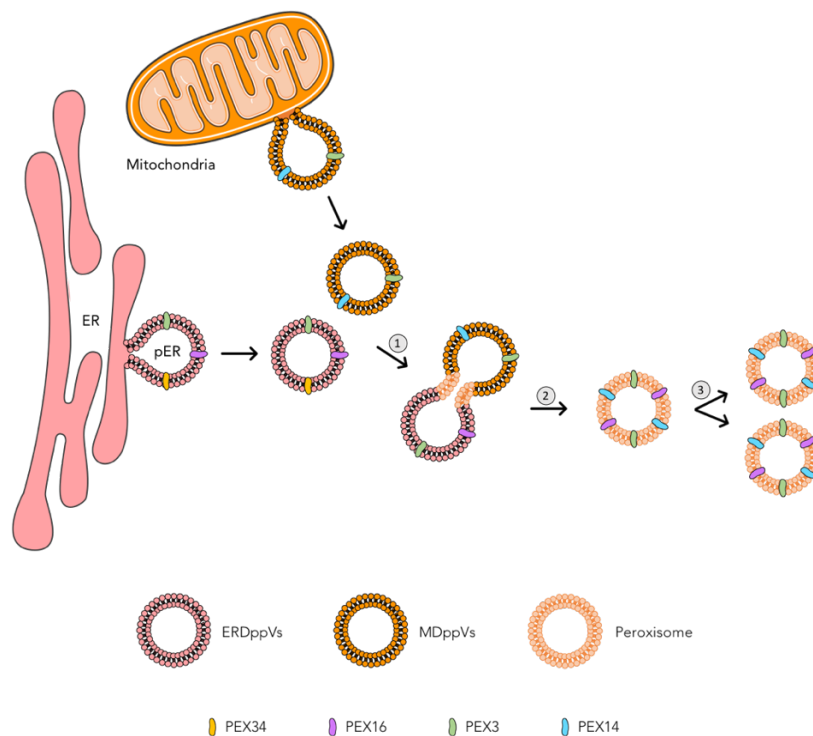


Figure 2. *De novo* model for peroxisome biogenesis. PMPs are imported to the membrane of the ER being afterwards sorted to specific regions, the pER, where the ppVs exit. There are two kinds of ppVs, ERDppVs, which are pre-vesicles derived from the ER, and MDppVs, that are mitochondria derived. It is most likely that the fusion of both ppVs happens making it possible the establishment of the competent peroxisomes. (1) – Fusion; (2) – Maturation; (3) – Fission; ER – Endoplasmic Reticulum.

| Peroxisomes Functions

Peroxisomes are multipurpose organelles essential for various functions that depend on the organism, cell type and the development stage of the organism^{3,30}. These organelles contain around 50 different enzymes indispensable for a diversity of metabolic pathways^{3,30}. Peroxisomes are important, e.g., for the biosynthesis of cholesterol, dolichol, inflammatory mediators, bile acids and β -oxidation of branched chain and very long-chain fatty acids. Besides that, peroxisomes are also crucial for the biosynthesis of glycerophospholipids such as plasmalogens. The three principal functions that stand out are: reactive oxygen species metabolism, ether lipid synthesis and fatty acid β -oxidation³².

| Oxygen Metabolism and Reactive Oxygen Species

Peroxisomes initially were described as organelles that could carry out oxidation reactions leading to the production of hydrogen peroxide (H_2O_2) through oxidases present in the organelle^{2,33}. However, since H_2O_2 is an extremely toxic and potentially pathogenic metabolite, peroxisomes acquire a way of restoring cellular homeostasis through the decomposition of H_2O_2 . This process may occur catalytically through catalase or peroxidatically where the conversion of hydrogen peroxide into two molecules of water (H_2O) is coupled to the oxidation of different hydrogen donors (AH_2) such as ethanol, methanol, formaldehyde, and nitrite (Figure 3)^{2,32-35}. If any small amount of H_2O_2 escapes from the peroxisomes they will encounter a secondary protective system, the glutathione peroxidase system, present in the cytosol, that will reduce H_2O_2 to H_2O protecting the organism from oxidative damage^{2,33,36}.

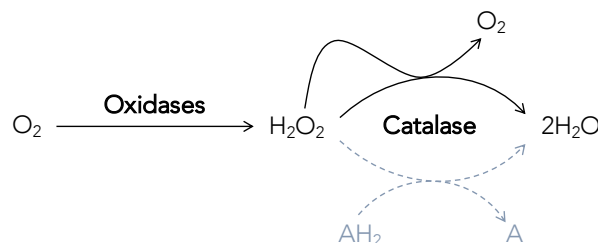


Figure 3. Oxygen metabolism and reactive oxygen species. First, there is the production of H_2O_2 through the oxidation of O_2 . Afterwards, since the H_2O_2 is toxic, its decomposition needs to occur. There are two different pathways: catalytically (black line) and peroxidatically (dashed line). The catalytically way decomposes H_2O_2

through catalase leading to the production of two molecules of H₂O and the release of O₂. The peroxidatically way decomposes H₂O₂ through the oxidation of various hydrogen donors leading to the production of two molecules of H₂O as well. O₂ – Oxygen; A – Donor.

| Ether Lipid Synthesis

Peroxisomes also play a crucial role in the biosynthesis of etherphospholipids (Figure 4). Briefly, the formation of ether lipids occurs in the luminal side of the peroxisome membrane and consists in the acylation of dihydroxyacetone phosphate (DHAP) at the sn-1 position by a glycerone phosphate O-acyltransferase (GNPAT), the transfer of acyl-DHAP across the enzyme active sites, followed by the exchange of the acyl group (fatty acid) for an alkyl group (fatty alcohol) by alkylglycerone phosphate synthase (AGPS)^{21,32,37,38}.



Figure 4. Ether lipid synthesis. The synthesis of ether lipids initiates with the acylation of DHAP by GNPAT leading to the formation of 1-acyl-DHAP. Afterwards, there is an exchange of the acyl group for an alkyl group by AGPS producing 1-O-alkyl-DHAP. 1-acyl-DHAP – 1-acyl-dihydroxyacetone phosphate; 1-O-alkyl-DHAP – 1-O-alkyl-dihydroxyacetone phosphate.

| Fatty Acid β -Oxidation

Another main role of peroxisomes is the β -oxidation of fatty acids. In normal conditions, the oxidation of medium and long-chain fatty acids is held essential by mitochondria³². However, there are several metabolites whose oxidation is strictly dependent on the activity of the peroxisomal β -oxidation system such as very long-chain fatty acids, pristanic acid, di- and trihydroxycholestanoic acid, tetracosanoic acid and long-chain dicarboxylic acids. The peroxisomal β -oxidation system is a transversal property of peroxisomes in most organisms and consists of 4 steps: (1) dehydrogenation, (2) hydratation, (3) dehydrogenation again and (4) thiolitic cleavage. Firstly, acyl-CoA is catalysed by acyl-CoA oxidase (ACOX) into enoyl-CoA followed by its conversion into 3-OH-acyl-CoA and, in turn, into 3-keto-acyl-CoA, both

catalysed by L- and D-bifunctional proteins, LBP and DBP, respectively. Lastly, 3-keto-acyl-CoA is converted into (n-2) acyl-CoA by 3-ketoacyl-CoA thiolase (ACAA1) or, as an alternative thiolase, the sterol carrier protein (SCP)^{21,32,38}.

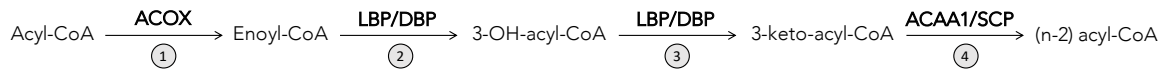


Figure 5. Fatty acid β -oxidation. The peroxisomal β -oxidation system can be divided into 4 steps: dehydrogenation, hydratation, dehydrogenation again and thiolytic cleavage. The first stage is performed by ACOX which converts acyl-CoA into enoyl-CoA. Next, the second and third stage are catalysed by two enzymes, LBP and DBP that are responsible for converting enoyl-CoA into 3-keto-acyl-CoA. Lastly, ACAA1 and SCP are the enzymes that convert 3-keto-acyl-CoA into (n-2) acyl-CoA. (1) – Dehydrogenation; (2) – Hydratation; (3) – Dehydrogenation; (4) – Thiolytic Cleavage.

| Peroxisomes and other organelles

In the past, it was thought that the different organelles were isolated entities with specific functions. However, it is now roundly accepted that there is a highly dynamic cooperative crosstalk and complex network of interactions between the subcellular compartments³⁹. These cooperative functions include not only metabolic interactions and intracellular signalling but also cellular maintenance, regulation of programmed cell death/survival and pathogen defense. These interactions can be established by vesicular transport, exchange of metabolites or signalling molecules through diffusion and direct physical contacts that are mediated by specialized membrane contact sites.

Peroxisomes have already been shown to cooperate with mitochondria, the ER, lysosomes and lipid droplets (Figure 6)^{39,40}.

| Peroxisomes and Mitochondria Interaction

Over the past decades, significant evidence for a close functional interplay between peroxisomes and mitochondria has been provided. Peroxisomes and mitochondria can be observed in close contact through ultrastructural studies in mammalian cells. However, the molecular background of physical interactions and their physiological relevance are still

scarce^{39,41,42}. Nonetheless, both organelles share or have complementary functions in several biosynthetic pathways and metabolic processes, including the breakdown of fatty acids, via their organelle-specific β -oxidation pathways in order to maintain lipid homeostasis; a redox-sensitive relationship that contributes to cellular reactive oxygen species (ROS) homeostasis; coordinated organellar biogenesis, by sharing key proteins of their division machinery; communication by a novel vesicular trafficking pathway, through the release of biological messengers such as ROS, lipids and other metabolites; and, more recently, it has also been demonstrated a cooperation in anti-viral signalling and defense (Figure 6)³⁹⁻⁴⁵. This "peroxisome-mitochondria interaction" indicates that these organelles do not exist in isolation and are dependent to each other for their function requiring coordinated biogenesis, turnover and inheritance. This means that peroxisomal alterations in metabolism, biogenesis, dynamics and proliferation can potentially influence mitochondrial functions and vice-versa^{39,41,43,45}.

| Peroxisomes and ER Interaction

The relationship between peroxisomes and the ER has been discussed as being implicated in the biosynthesis of ether-phospholipids, that starts in peroxisomes and is completed in the ER, the biosynthesis of polyunsaturated fatty acids, and the formation of glycosyl phosphatidyl inositol (GPI)-anchored proteins in the ER^{40,45,46}. Peroxisomes depend on the ER for their lipid composition and, besides that, there is also an exchange of precursors between these two organelles. ER provides some membrane proteins to peroxisomes and peroxisomes also deliver lipid precursors required for the biosynthesis of specialized lipids of the ER. More recently, although controversial, it was shown that the ER plays a role in the biogenesis of peroxisomes, as well as in regulating their function⁴⁶. All things considered, the peroxisome-ER interaction, according to protein composition and physiological function, although still ambiguous, can be associated with two cellular processes: the exchange of metabolites from shared biochemical pathways and the biogenesis of peroxisomes (Figure 6)^{39,40,45,46}.

| *Peroxisomes and Lysosomes Interaction*

Cholesterol is an essential lipid for eukaryotic cells and plays an essential role in several cellular processes such as membrane properties regulation, bile acid synthesis, and signal transduction. In recent studies, it was shown that peroxisomes form membrane contacts with lysosomes (LPMC) that are indispensable for the intra-cellular cholesterol transport from lysosomes to peroxisomes (Figure 6). Furthermore, some authors believe that intracellular cholesterol accumulation may underlie pathological mechanisms of peroxisome disorders which means that this interaction is fundamental for the proper functioning of the cell^{39,47,48}.

| *Peroxisomes and Lipid Droplets Interaction*

Lipid droplets (LD), also termed "lipid particles", "lipid bodies" or "oil bodies", are dynamic ubiquitous subcellular structures involved in multiple cellular processes such as the storage of neutral lipids, mainly triacylglycerols (TAG) and sterol esters (SE), for energy and membrane homeostasis⁴⁹. However, they are also involved in protein sequestration/degradation and pathogen replication. These LD are being more and more recognized as metabolically highly dynamic organelles with increased biomedical interest. Peroxisomes are often found in close association with LDs and it was shown that they stably adhere to lipid bodies. This interaction results in the synthesis of free fatty acids from neutral lipids providing a substrate for peroxisomal fatty acid β -oxidation which means that a transfer of fatty acids from the lipid body to the peroxisome may occur across the organellar boundaries. Furthermore, exchange of lipids between these two organelles may also serve as a membrane replenishment or storage in LDs (Figure 6)^{39,49-52}.

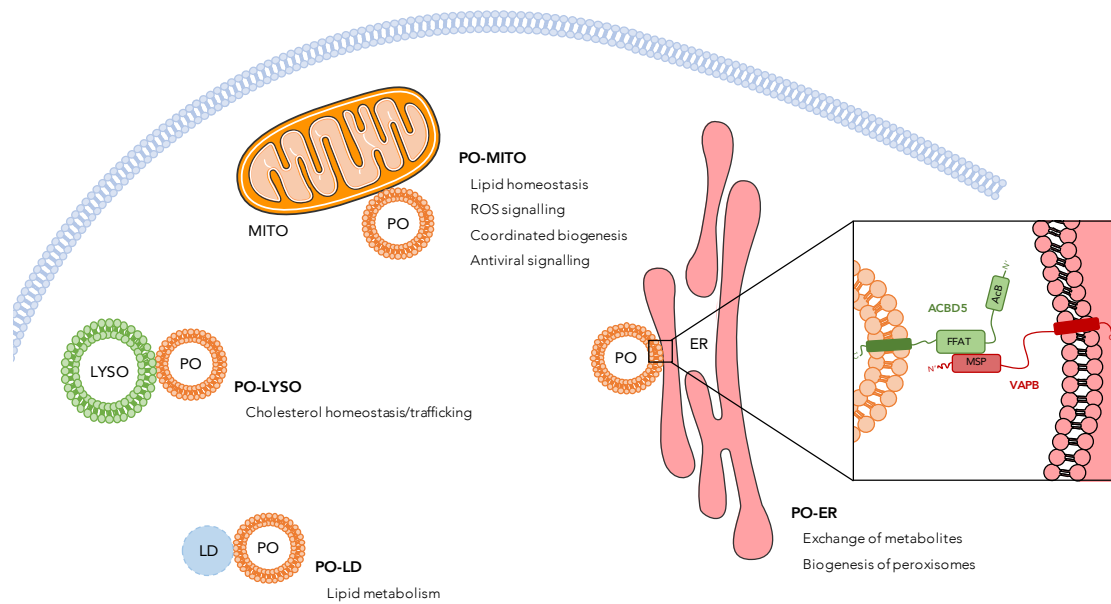


Figure 6. Peroxisomes and their interaction with other organelles. Schematic diagram of the interactions between peroxisomes with other organelles in mammals. PO – Peroxisomes; MITO – Mitochondria; LYSO – Lysosomes; ER – Endoplasmic Reticulum; ACBD5 – Acyl-CoA binding domain protein 5; FFAT – Two phenylalanine in an acidic tract; ACB – Acyl-coenzyme A-binding domain; VAPB - Vesicle-associated membrane protein-associated protein B; MSP – Major sperm protein; N' – N terminal; C' – C-terminal.

1.2 | Cellular Antiviral Signalling

The immune system is found in most multicellular organisms and is characterized by the capacity of resistance to infection or disease, protecting it from infectious and potentially pathogenic agents^{53,54}. This system, comprising innate and adaptive immune responses, recognizes the presence of these agents and respond properly to contain or eliminate the threat, in order to recover the homeostasis of the organism. In a context of infection, the innate immune system is the first line of host defense against infection, having an essential role in the early recognition of pathogens and in triggering the proinflammatory responses, whereas the adaptive immune system appears in a latter phase of infection and is responsible for the elimination of pathogens and for the immunological memory in general^{53,54}. The innate immune response is considered non-specific, being constituted mainly by physical and chemical barriers to infection and different antigen-presenting cells (APCs), such as granulocytes, macrophages and dendritic cells (DCs). The activation of the innate immunity is mainly through different host pattern recognition receptors (PRRs) which recognize pathogen associated molecular patterns (PAMPs). Consequently, PRR-induced signalling transduction pathways are activated, inducing gene expression and synthesis of a variety of molecules, including cytokines, chemokines, and immunoreceptors, that will cooperate in order to stimulate the early host response and allow the latter activation of the adaptive immune response^{53,55–57}.

There are various PRRs that can be categorized according to their location, ligand specificity and functions. Regarding on their cellular location, PRRs can be bound to a membrane, which include Toll-like receptors (TLRs) and C-type lectin receptors (CLRs), or free in the cytosol, which comprise nucleotide-binding oligomerization domain (NOD)-like receptors (NLRs), retinoic acid-inducible gene-I (RIG-I)-like receptors (RLRs) and, cytosolic viral DNA sensors such as cyclic guanosine monophosphate-adenosine monophosphate (cGAMP) synthase (cGAS). Accordingly, the location of PRRs allows the differentiation between the various PAMPs and, consequently, the activation of the correct downstream signalling molecules and corresponding signalling cascades^{58–64}.

| Toll-like receptors

The TLRs are the most studied PRRs being considered the primary sensors of pathogens with a critical role in the innate and adaptive immune response. TLRs are mainly divided into two groups depending on their cellular localization and respective PAMP ligands. One group, composed of TLR1, TLR2, TLR4, TLR5, TLR6 and TLR11, is localized on cell surfaces and can recognize microbial membrane components such as lipids, lipoproteins and proteins. The other group, composed of TLR3, TLR7, TLR8 and TLR9, is expressed exclusively within intracellular vesicles, such as the ER, endosomes, lysosomes and endolysosomes, where it recognizes microbial nucleic acids. More recently, it was shown that TLR11 besides being expressed on the cell surface, is also expressed in intracellular compartments (Figure 7)^{59,61–63,65,66}.

TLRs are type I membrane glycoproteins with an N-terminal extracellular domain (ECD), a single transmembrane helix and a carboxy-terminal cytoplasmic Toll/Interleukin (IL)-1 receptor (TIR) domain^{59–65,67}.

TLR signalling initiates once the ligand binds to this receptor (Figure 7). This contact promotes interactions between TLRs leading, consequently, to the dimerization of the TIR domain. The dimerized TIRs will serve as a platform to recruit different cytosolic adaptor proteins such as Myeloid differentiation primary response gene 88 (MyD88), TIR-domain-containing adaptor inducing interferon β (TRIF), TIR domain-containing adaptor protein (TIRAP) and TRIF-related adaptor molecule (TRAM), all of them containing also TIR domains. Accordingly, and depending on the nature of the adaptor, this recruitment will activate numerous transcription factors, namely Nuclear factor kappa B (NF- κ B), Interferon regulatory factor 3 (IRF3), Interferon regulatory factor 7 (IRF7) and Mitogen-activated protein kinases (MAPK), that in turn will culminate in the production of pro-inflammatory cytokines, chemokines and type I interferons (IFNs) and also influence cellular maturation and survival (Figure 7)^{59–65,67}.

The individual TLRs activate specific biological responses according to the various PAMPs, derived from bacteria, viruses, fungi and parasites that are detected by these receptors and

deregulations from these signalling cascades can give rise to several diseases including important autoimmune diseases^{61,63}.

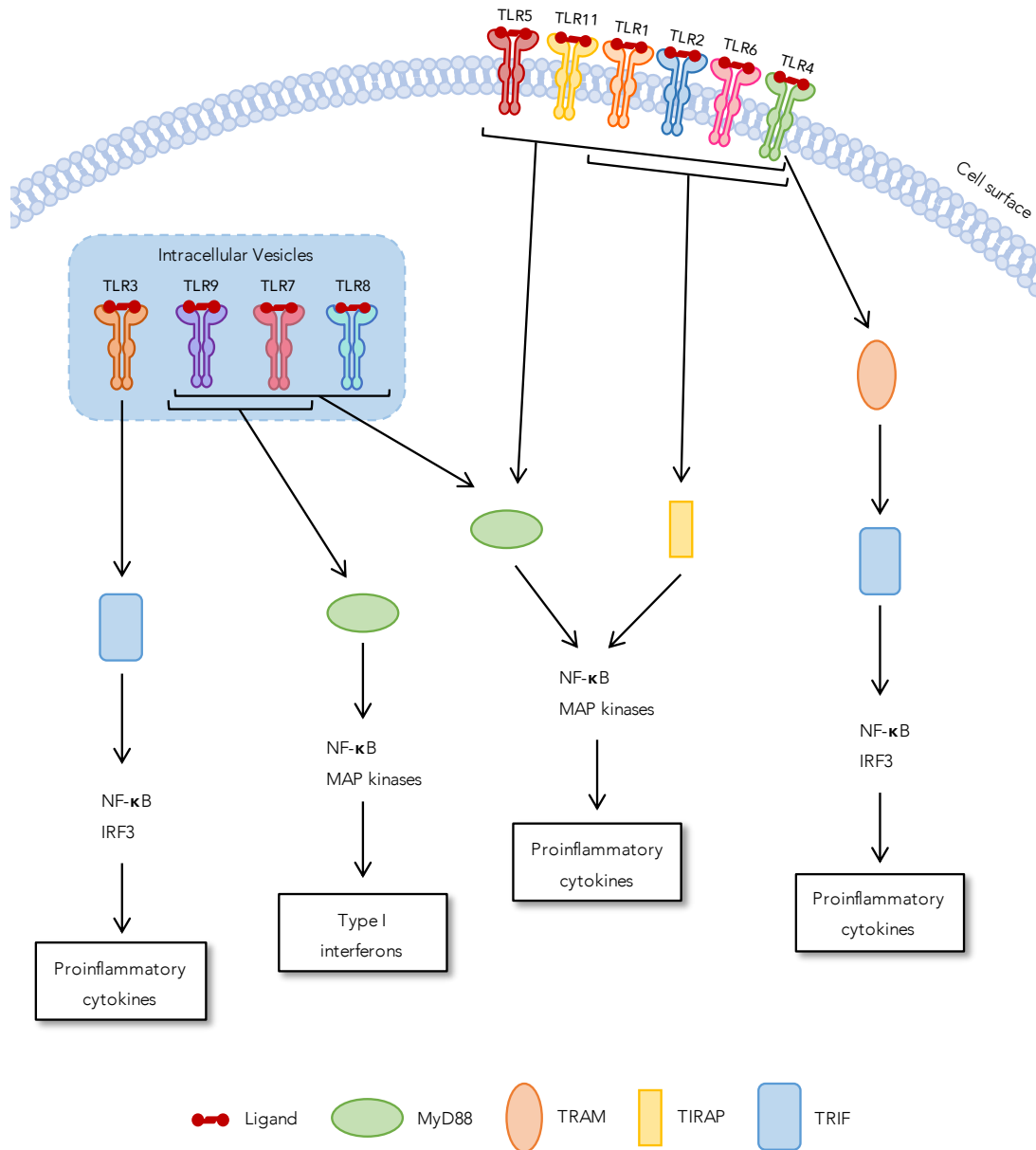


Figure 7. TLRs signalling. TLRs can be divided into two different groups: localized on the cell surface and localize on intracellular vesicles. All of them, except TLR3, recruit MyD88 which in turn activates NF-κB and MAP kinases which then recruit proinflammatory cytokines. TLR1, TLR2, TLR4 and TLR6 can also recruit TIRAP that will activate the same pathway as MyD88. TLR3 is responsible for the recruitment of TRIF that will activate NF-κB and IRF3 that recruit also proinflammatory cytokines. Furthermore, TLR4 can also recruit the TRIF pathway through TRAM. To note, TLR7 and TLR9 are responsible for the activation of type I interferons.

| Cytosolic DNA sensors

Sun et al.⁶⁸, through biochemical approaches, demonstrated that cyclic GMP-AMP synthase (cGAS) binds directly to intracellular DNA and synthesizes cyclic GMP-AMP (cGAMP), from GTP and ATP, functioning as a second messenger in response to intracellular DNAs activating the stimulator of interferon genes (STING). Prior to the discovery of cGAS other proteins were suggested to function as DNA sensors, such as DNA-dependent activator of IFN-regulatory factors (DAI), IFN- γ -inducible protein 16 (IFI16), DNA-dependent RNA polymerase III (Pol III), absent in melanoma 2 (AIM2), among others⁶⁹⁻⁷¹.

cGAS is involved in immune responses against viral and bacterial DNA, retrovirus infection, and self-DNA which includes mitochondrial dsDNA and intracellular bacteria. This sensor cannot distinguish between self- and non-self-dsDNA meaning that the same mechanisms are activated for both of them⁶⁹⁻⁷².

The cGAS-mediated signalling pathway begins after the binding of the DNA to the cGAS (Figure 8). This sensor contains two positively charged DNA binding sites and a principal single groove that includes an activation site for synthesizing cGAMP. In the absence of DNA, cGAS remains in an autoinhibited state and, when binding to DNA undergoes conformational changes, leading to the exposure of the activation site which, in turn, will catalyse the synthesis of cGAMP, from ATP and GTP, that will subsequently bind to STING (Figure 8). STING then traffics from the ER to an ER-Golgi intermediate compartment (ERGIC) and the Golgi apparatus, which is an essential process to activate the downstream signalling by recruiting both IKK complex and TBK1. This will induce the activation and translocation of NF- κ B and IRF3 into the nucleus, which induce the expression of IFNs and inflammatory cytokines, such as TNF, IL-1 β and IL-6 (Figure 8). Moreover, the cGAS and STING activities can be also regulated by post-transcriptional modifications, for instance phosphorylation and polyubiquitination, respectively^{68,71,72}.

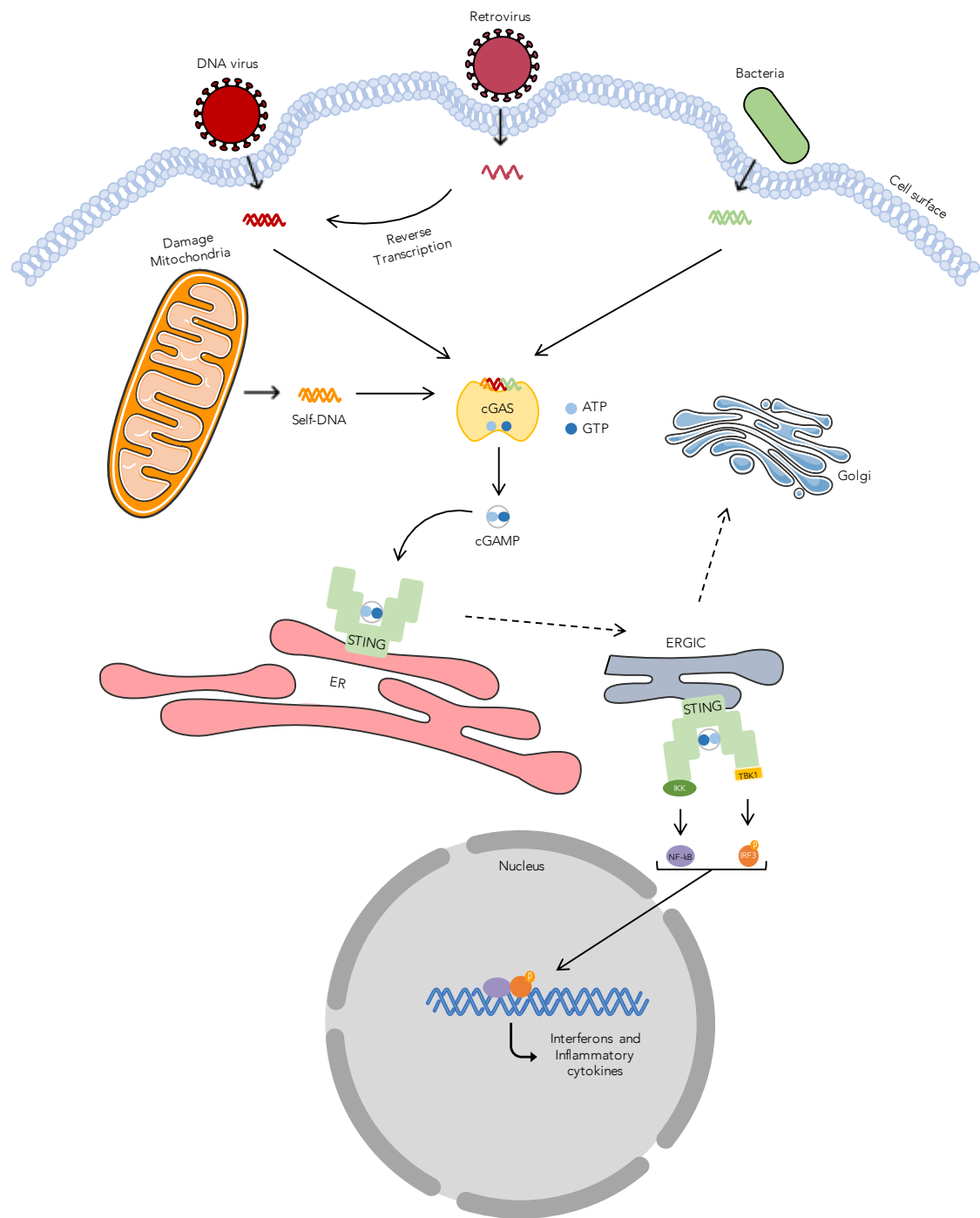


Figure 8. cGAS-mediated signalling. cGAS is involved in response against retrovirus infection, DNA infection, self-DNA and bacterial DNA. After the binding of the DNA cGAS allows the synthesis of cGAMP from ATP and GTP which in turn will bound to STING. STING traffics from the ER to an ER-Golgi intermediate compartment and then to the Golgi apparatus. Once in the ERGIC, STING recruits TBK1 and IKK which in turn will recruit and activate NF-κB and IRF3. Both of them are translocated into the nucleus which induces the expression of interferons and inflammatory cytokines.

| RIG-I like receptors

The RLR family of receptors recognizes viral RNA at the cytoplasm and consists of three members: retinoic acid inducible gene I (RIG-I), melanoma differentiation associated gene 5 (MDA5) and laboratory of genetics and physiology 2 (LGP2). RIG-I and MDA5 are constituted by two tandem N-terminal caspase activation and recruitment domains (CARDs) followed by a DExD/H-box RNA helicase domain with an ATPase activity and, lastly, a C-terminal domain (CTD). The CARDs have an essential role in autorepression and signalling, moreover, they are responsible for the transmission of the activation signal downstream. The CTD is responsible for the binding of the viral nucleic acid. The principal difference between RIG-I and MDA5 is their crystal structure. MDA5 CTD is rotated, bringing the viral nucleic acid closer in comparison with the RIG-I structure. Unlike RIG-I and MDA5, LGP2 lacks the CARD domains containing only the helicase domain. This suggests a negative regulatory role in RIG-I and MDA5-mediated signalling. However, recent studies also suggest that LGP2 acts as a positive regulator^{58,60,67,73,74}.

All of these cytoplasmic receptors are vastly expressed in most tissues, playing an important role in triggering innate defences within a variety of cell types. The immune responses are triggered in response to RLRs recognition of different PAMPs. RIG-I recognizes some negative-sense single-stranded RNA viruses, such as the vesicular stomatitis virus (VSV), influenza A virus (IAV) and Newcastle disease virus (NDV); positive-sense single-stranded RNA viruses, for example hepatitis C virus (HCV); and also recognizes short double-stranded RNA (up to 1kb) with triphosphate or monophosphate at 5' end^{57,59,66,67,75}. On the other hand, MDA5 recognizes some positive-sense single-stranded RNA viruses as well. Additionally, some viruses such as dengue virus (DENV) and West Nile virus (WNV), require the recognition of both receptors, RIG-I and MDA5, with the purpose of generating a robust response⁷⁴. The third member of the RLR family, LGP2, is less understood. Nonetheless, it is thought that LGP2 recognizes the termini of dsRNA through similar types of protein-RNA contacts as RIG-I and MDA5^{57,59,66,67,75,76}. Through various experimental approaches, and as was previously said, LGP2 has been considered to be both negatively and positively regulator of RIG-I and MDA5 signalling, respectively. This happens because LGP2

competitively recognizes the viral ligand the same way as RIG-I, downregulating the signalling pathway of this receptor. On the other hand, LGP2 also enhances MDA5 signalling through mechanisms that still remain unclear. Consequently, after a viral stimuli LGP2 affects the signalling response by modulating both RIG-I and MDA5 signals (Figure 9)^{57,67,73,76}.

The RLR signalling pathway initiates in the cytoplasm where RIG-I and MDA5, along with LGP2, sense the viral nucleic acids inducing conformational rearrangements which convert them from an auto-repressed state into a full competent signalling state (Figure 9). In the auto-inhibited state of the receptor RIG-I, its helicase has an open and flexible state with low affinity for ATP and the ligand. On the other hand, the CTD is bound to the bridging helix by a flexible linker remaining this way available for sensing and capturing PAMPs with high affinity. Hence, viral nucleic acid binds to the CTD, leading to conformational changes that will force the exposure of the CARDs becoming potentially available for downstream interactions. This exposure on 55-residue-long in the N-terminal makes them accessible for K63-linked polyubiquitination or polyubiquitin binding of CARD2 at Lys172. Moreover, the CARD domains recruit TRIM25, an E3 ubiquitin ligase, and other ubiquitination enzymes to synthesize unanchored K63 polyubiquitin chains which will bound to the CARD domains. The TRIM25-mediated ubiquitination of RIG-I may then facilitate its interaction with MAVS. After polyubiquitination, downstream signalling via MAVS can finally occur. Upon recognition of the viral genome, although via a distinct mechanism, MDA5 also interacts with mitochondrial MAVS for further downstream signalling. On the other hand, since it lacks CARDs domains, LGP2 does not interact with MAVS, affecting this signalling pathway only through the modulation of the signals from RIG-I and MDA5 (Figure 9)^{58,73,76-83}.

MAVS is localized at the membranes of mitochondria, peroxisomes and mitochondria associated membranes (MAM) and is composed of an N-terminal CARD domain, a central proline-rich region, and a C-terminal transmembrane domain. After being activated by RIG-I and MDA5, it occurs the formation of a macromolecule complex. Subsequently, the protein-interacting CARDs of both proteins lead to the formation of prion-like aggregates of the CARD domain of MAVS, which ultimately convert other MAVS molecules into functional aggregates, in a highly processive manner (Figure 9)^{58,73,76-83}.

Activated MAVS on the mitochondrial surface interact with each other through both intra and inter-strand interfaces between their CARD domains, resulting in rod-shaped clustered MAVS aggregates that may contain MAVS molecules from multiple mitochondria. These molecular aggregates act like prion fibers, since they are detergent-resistant, protease-resistant and self-perpetuating by inducing inactive MAVS to form functional aggregates. Although these prion-like filaments have all the properties of other prion proteins, they use different chemistry which leads to a gain of function and, consequently, to efficient and tightly regulated signalling. It was also demonstrated that the N-terminal CARD domain of MAVS is necessary and sufficient for the formation of active MAVS aggregates and that the transmembrane domain is the main determinant of the self-interaction^{80,81,84-89}.

After oligomerization, and once MAVS contains specific regions that are TNF receptor-associated factor (TRAF) interacting motifs (TIMs), it occurs the recruitment of TRAFs, suggesting that there is an induction of antiviral responses through TRAFs (Figure 9). There are four members of the TRAF family that can be recruited, TRAF2, 3, 6 and 5. TRAF3 is required for the activation of TBK1 while TRAF2, TRAF5 and TRAF6 activate IKK and NF- κ B. The polymerization of MAVS increases the affinity of the interaction MAVS-TRAFs, resulting in the recruitment and activation of TRAFs proteins, which might lead to the oligomerization of the TRAFs and, consequently, to the activation of their ubiquitin E3 ligase activity (Figure 9)^{80,81,84-89}. Notably, the interaction between MAVS and TRAF proteins depends not only on viral PAMPs recognition but also in MAVS polymerization. According to Liu *et al.*⁵⁸, a specific mutation in the CARD domain of MAVS that allows the disruption of its polymerization can completely abolish the recruitment of TRAFs. The activation of the ubiquitin E3 ligase activity of TRAFs leads to the production of ubiquitin chains that will bind and activate NEMO which in turn activates IKK α / β and will also allow the interaction of TBK1/IKK ϵ and the consequent formation of a complex that will be recruited to the complex MAVS-TRAFs (Figure 9). The IKK complex is essential for the full activation of this pathway and is constituted by three components, IKK α , IKK β and NEMO. These IKK are responsible for the full activation of TBK1/IKK ϵ that is now in the cytosol to further activate IRF3/7 through phosphorylation (Figure 9). After that, they undergo autophosphorylation and are recognized via the ubiquitin chains produced by TRAFs, leading to their

polyubiquitination and subsequent proteasomal degradation, which leads ultimately to the freed of NF- κ B. Both IRF3/7 and NF- κ B bind to the IFN β promoter in a temporal manner, leading to its transcription (Figure 9). The secreted IFN β then binds to and activates the type I IFN receptor in an autocrine or paracrine manner and this ligand-receptor interaction allows the activation of the JAK-STAT pathway as well as the formation of ISGs that will further function as direct antiviral effectors, acting to prevent viral genome replication, viral particle assembly, or virion release from infected cells (Figure 9)^{84,86,90–99}.

The signalling pathway downstream peroxisomal MAVS is still poorly understood. The oligomerization of MAVS has been observed (data not published) and the activation of IRF3 and IRF1, that will then bound to the IFN λ promoter, leading to its transcription have been demonstrated¹⁰⁰. The secreted IFN λ binds and activates the type I and III IFN receptor to allow the activation of the JAK-STAT pathway and the formation of ISGs (Figure 9). According to Dixit *et al.*¹⁰⁰, the peroxisomal localization of MAVS is required for rapid but transient induction of antiviral ISGs, whereas mitochondrial MAVS promotes a stable ISG expression with delayed kinetics, suggesting that important differences may exist between the signalling pathways originating from these two different organelles^{8,100–104}.

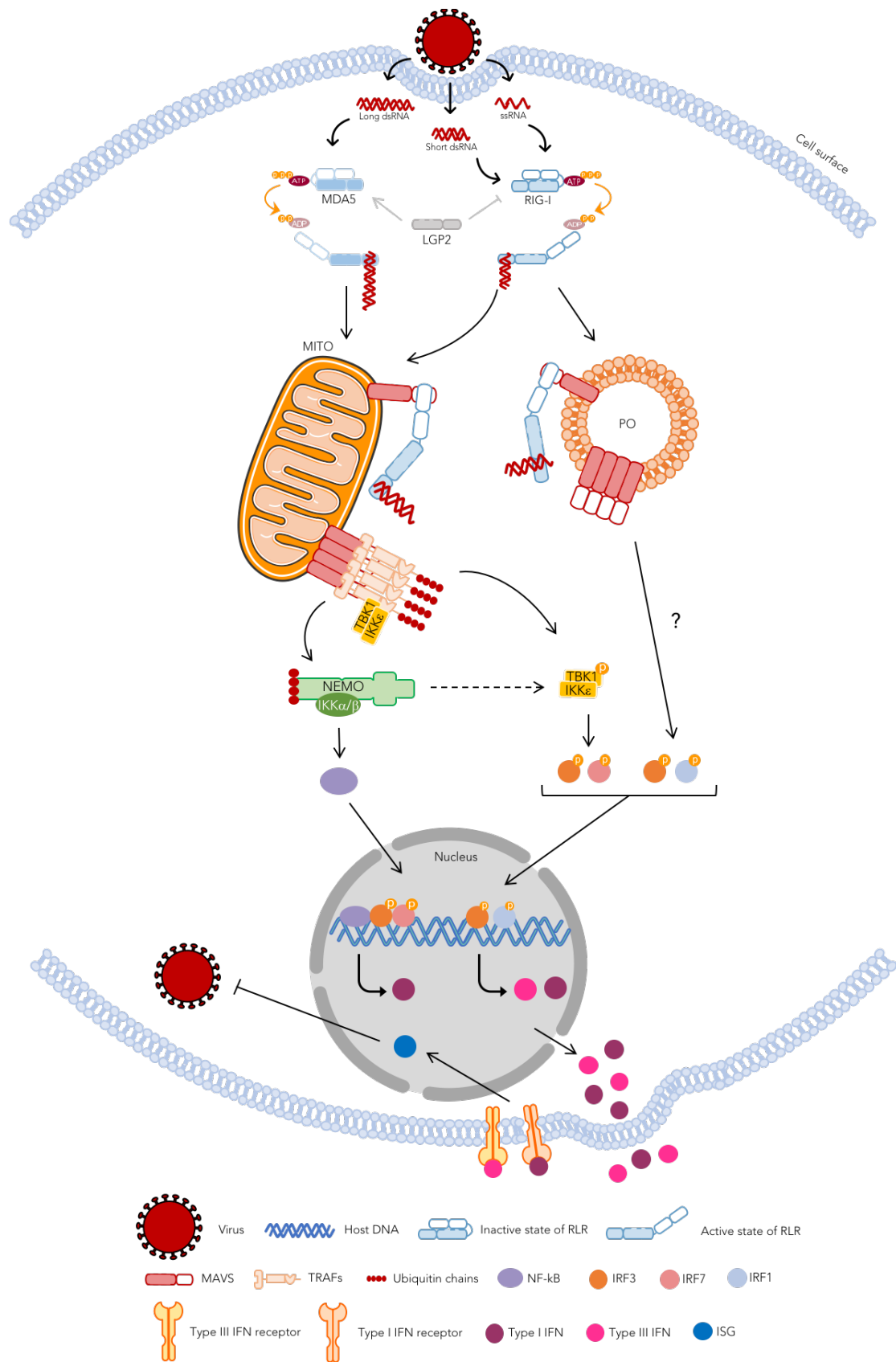


Figure 9. RLR signalling. Upon viral infection, the viral nucleic acid promotes the activation of the RLRs. More specifically, long dsRNA activates the MDA5 receptor and, short dsRNA and ssRNA activates the RIG-I receptor.

Afterwards, these receptors suffer conformational changes allowing the activation of MAVS which oligomerizes and induces a signalling cascade which ultimately leads to the activation of the JAK-STAT pathway and formation of ISGs that function as direct antiviral effectors, acting to prevent viral genome replication, viral particle assembly, or virion release from infected cells. This signalling process is under tight regulation and dependent on post-translational modifications of RIG-I and MDA5 and also on regulatory proteins which include the third RLR, LGP2. MITO – Mitochondria; PO – Peroxisome.

II. Aims

Upon infection, the viral genome is recognized by the cellular machinery leading to the initiation of a signalling cascade that culminates with the production of antiviral effectors which prevent important virus propagation. Peroxisomes and mitochondria have been shown to act in concert as important signalling platforms within the cellular antiviral response. Although the mitochondrial signalling pathway is well established, the exact steps that constitute and distinguish the peroxisomal signalling pathway are still unknown.

The main goal of this project is to unravel the peroxisomal MAVS-dependent signalling pathway. To that end, we proposed to use two viral proteins that are known to hamper the mitochondrial-dependent antiviral response at specific steps of the signalling pathway and investigate their effect on the peroxisome-dependent signalling.

III. Materials and Methods

3.1 | Materials

| Cell lines

MEFs MAVS-PEX | Mouse Embryonic Fibroblasts with MAVS only at peroxisomes^{105,100}

| Cell Culture Solutions

Dulbecco's Modified Eagle Medium (DMEM) High Glucose w/L-Glutamine w/o Sodium Pyruvate	Gibco
Fetal Bovine Serum (FBS), qualified, E.U.-approved, South America origin	Gibco
Penicillin/Streptomycin	Gibco
Dulbecco's Phosphate Buffered Saline w/o Calcium w/o Magnesium	Gibco
Trypsin-EDTA 1x in PBS w/o Calcium w/o Magnesium w/o Phenol Red	Gibco
Lipofectamine 3000	Invitrogen
P3000	Invitrogen
Opti-Mem Reduced-Serum Medium (1x)	Gibco

| Plasmids

Table 1. List of plasmids.

Plasmid	Tag	Antibiotic Resistance	Manufacture
pEGFP-C1-RIG-I-CARD	GFP	KAN	Given by Dr. Friedmann Weber, Justus Liebig University
HA-NP	HA	AMP	Given by Dr. Stefan Kunz, Institute of Microbiology University Hospital Center and University of Lausanne
UL36-YFP	YFP	KAN	Given by Dr. Chunfu Zheng, Institutes of Biology and Medical Sciences

| Primers and Oligonucleotides

Table 2. List of PCR primers.

PCR primers			Manufacture
IRF1	IRF1 mouse	Forward 5' GGTCAGGATTGGATATGGA 3' Reverse 5' AGTGGTGCTATCTGGTATAATGT 3'	Eurofins
GAPDH	GAPDH mouse	Forward 5' AGTATGTCGTGGATCTA 3' Reverse 5' CAATCTTGAGTGAGTTGTC 3'	Eurofins

| Transfection Reagents

Lipofectamine 3000

Invitrogen

| Markers and Loading Dyes

Table 3. List of markers and loading dyes.

Markers	Reagents	Manufacture
6x Laemmli Buffer	350mM Tris pH 6,80	Thermo Fisher
	10mM Sodium Dodecyl Sulfate (SDS)	Fisher Scientific
	60mM dithiothreitol (DTT)	NewEngland Biolabs
	0.06% Bromophenol Blue	Sigma-Aldrich
GRS Protein Marker Multicolour Tris-Glicine		Grisp
O' Gene Ruler DNA Ladder Mix		Thermo Fisher
6x Orange DNA Loading Dye		Thermo Fisher

| Antibodies

Table 4. List of primary antibodies.

Primary	Species	Production	Dilution		Company
			WB	IMF	
Tubulin	Mouse	Monoclonal	1:1000		Sigma-Aldrich
PMP70	Mouse	Monoclonal		1:200	Sigma-Aldrich
HA	Rabbit	Polyclonal	1:100		Clontech
p-STAT1	Mouse	Monoclonal	1:1000		Bio-legend

Table 5. List of secondary antibodies.

Secondary	Species	Production	Dilution		Company
			WB	IMF	
IRDye®680CW	Mouse	Polyclonal	1:10 000		LI-COR
IRDye®800CW	Rabbit	IgG (H+L)	1:10 000		LI-COR
TRITC 561	Mouse			1:100	Invitrogen-Molecular Probes

| Solutions and Buffers

Table 6. List of solutions and buffers.

Solutions	Reagents	Manufacture
Ammonium Persulfate (APS)	0.2% APS	Sigma-Aldrich
Blotting Buffer	48mM Tris Base	Fisher Scientific
	39mM Glycine	Fisher Scientific
	0.04% SDS	Fisher Scientific
	20% MeOH	Merck Milipore
Bovine Serum Albumine (BSA)		NZYTEch
Mowiol	¾ Mowiol	Apply Chem
	¼ n-propyl-Gallat	Sigma-Aldrich
Loading Buffer	1M Tris pH 6,80	Thermo Fisher
	10% Glycerol	
	1M DTT	
	20% SDS	
	β-Mercaptoethanol	
	0.1% Bromophenol Blue	Sigma-Aldrich

Milk for Blot blocking	5g of powder milk	Nestle
	100mL 1x TBS-T	
Paraformaldehyde (PFA)		Sigma-Aldrich
10x TBS-T	100mM Tris Base	Fisher Scientific
	1.5M NaCl	ACROS
	0.05% Tween 20	Sigma-Aldrich
10x PBS	1.369M NaCl	ACROS
	0.0268M KCl	Sigma-Aldrich
	80mM Na ₂ HPO ₄	Sigma-Aldrich
	0.0147M KH ₂ PO ₄	Sigma-Aldrich
10x SDS – Running Buffer	250mM Tris	Fisher Scientific
	1.9M Glycine	Fisher Scientific
	20% SDS	Fisher Scientific
50x TAE	0.04M Tris-HCl	Fisher Scientific
	0.02M Acetic-acid	Merck Milipore
	1mM EDTA	Sigma-Aldrich
0.2% Triton X-100	0.2% Triton X-100	
	1x PBS	
Trizol		

| Databases and Software's

- Excel, Microsoft;
- Image Lab, Bio-Rad;
- Image Studio Software for Odyssey;
- National Center for Biotechnology Information (NCBI);
- UNIPROT;
- AxioVision Software

| Equipment

- CO2 incubator MCO-17AIC, Sanyo;
- Pipettes Eppendorf Research, Eppendorf;
- My Cyclor Thermal Cyclor, Bio-Rad;
- 7500 Real-Time PCR System, Applied Biosystems;
- Nanodrop (DeNovix);
- Mini Protean Tetra Cell (Bio-Rad);
- Mini Trans-Blot® Electrophoretic Transfer Cell (Bio-Rad);
- Odyssey, LI-COR;
- ChemiDoc, BioRad;
- Zeiss Confocal LSM 510M;
- Gel Doc, BioRad.

3.2 | Methods

| Cell culture

| *Cell lines maintenance*

In order to perform the present work, the cell lines Mouse Embryonic Fibroblasts that express MAVS solely at peroxisomes (MEFs MAVS-PEX cells) were used, which was kindly provided by Dr. Kagan from Harvard Medical School^{100,105}.

The cell lines were routinely cultured and split twice a week in a 100cm culture dishes, after reaching approximately 80% of confluency, with high glucose DMEM supplemented with 10% of FBS and 1% of Penicillin/Streptomycin, named as complete DMEM. The cells were then maintained in culture at 37°C in a humidified atmosphere containing 5% CO₂. For cells splitting, the confluent cells were washed one time with 1x PBS and incubated with 1x trypsin-EDTA at 37°C and 5% CO₂. When individual cells become separated and detached from the dish surface, cells were resuspended in complete DMEM and centrifuge at 1000 g for 3 minutes at room temperature. Afterwards, the supernatant was discarded, and the pellet was resuspended in 10mL of complete DMEM. From this, the cells can either be divided according to experimental procedures and/or seeded in a 1:10 dilution.

| *Cell storage, freezing and thawing*

Cells stocks were prepared from 80-90% confluent cells resuspended in DMEM with 10% of FBS and 10% of DMSO and were kept in cryovials aliquots of 1.5mL. Stocks were frozen in -80°C before being placed in the liquid nitrogen tank for cryopreservation.

When needed, frozen cells were thawed through resuspension with pre-warmed complete DMEM and seeded in a 100cm culture dishes. After cell adhesion, approximately 6 hours, the medium was replaced by fresh growth medium in order to eliminate cell debris and the DMSO that is toxic for cells.

| Transient Mammalian Transfection Methods

| *Lipofectamine 3000*

Lipofectamine 3000 protocol was performed on MEFs MAVS-PEX cells. In this cationic lipid-mediated method, the negatively charged DNA binds spontaneously to the positively charged liposomes forming DNA cationic lipid reagent complexes. To prepare these plasmid DNA-lipid complexes, the transfectable DNA together with P3000 reagent (1:1 ratio) was diluted in Opti-MEM and, alongside, the Lipofectamine 3000 was also diluted in Opti-MEM. The solution of Lipofectamine 3000/Opti-MEM was then added to the diluted DNA/P3000 and incubated for 15 minutes at room temperature. Previously to adding the mixture dropwise to the cells, the growth media was changed to fresh complete media. Afterwards, cells were incubated at 37°C in a humidified atmosphere containing 5% CO₂ for the desired time. This procedure was used to transfect HA-NP and UL36-YFP into MEFs MAVS PEX and GFP-RIG-I-CARD into MEFs MAVS PEX.

| Immunofluorescence

To perform the immunofluorescence assay, 12ømm glass coverslips were added to the plates before seeding cells. After the transfection assays, the coverslips were washed 3 times with 1x PBS, fixed with 4% paraformaldehyde (PFA) for 20 minutes, permeabilized with 0.2% Triton X-100 for 10 minutes and blocked with 1% BSA for 10 minutes, being all the procedures performed at room temperature.

Afterwards, cells were stained with 20µL of the primary antibody for 1 hour in a humid environment, and with the secondary antibody for 1 hour in a humid environment protected from the light. Next, the coverslips were incubated with 20µL of DAPI for 3 minutes. All the incubations were performed at room temperature and between each step the cells were washed 3 times with PBS.

Finally, the coverslips were washed in double-distillated water, mounted in proper glass slides with mounting medium, Mowiol, that allows the adhesion of the coverslip on the slide. The slides were stored at 4°C in the dark until observation under a fluorescence or a confocal microscope.

The cells were observed with Zeiss LSM 510 confocal microscope, using a Plan-Apochromat 63x and 100x/1.4 NA oil objectives and ZEN Software. The lasers used were 488 nm Argon-ion laser, 561 nm DPSS laser and 405 nm HeNe for samples stained with GFP, TRITC and DAPI, respectively.

| RT-qPCR

| *Isolation of RNA*

Cells in the well plate were washed with 1x PBS and lysed at room temperature with 500 μ L of Trizol. After being harvested by pipetting up and down, the samples were collected and stored at -80°C. When needed, samples should be thawed and incubated for 5 minutes at room temperature.

In order to obtain a fractionated solution of cellular content, 100 μ L chloroform was added, the samples were shaken vigorously for 15 seconds and incubated for 5 minutes at room temperature. Following centrifugation of 15 minutes at 12 000 g at 4°C, a phase-separation occurred and the upper aqueous phase containing the RNA was collected into a new tube. This RNA was incubated on ice with 250 μ L of isopropanol for 10 minutes and then centrifuged for 15 minutes at 12 000 g at 4°C. The supernatant was removed, and the pellet was washed twice with 500 μ L of 75% ethanol interspersed by maximum speed centrifugation at 4°C for 5 minutes. After removing the ethanol, the pellet was dried for 10 minutes and further was resuspended with 20 μ L of RNase free water (pre-heated at 55°C) and incubated at 55°C for 10 minutes. The RNA concentration was measured with the Nanodrop equipment and the RNA was stored at -80°C.

| *cDNA synthesis*

cDNA synthesis was accomplished by mixing 1 μ g of the extracted RNA with a master mix of 280pmol of Oligo-dT primer, 166 μ M dNTPs, 1x M-MuL V Reverse transcriptase buffer, 100U M-MuL V Reverse transcriptase, 20U RNase inhibitor and RNase free water making a final volume of 30 μ L. The mixture was well mixed and incubated for 10 minutes at room temperature. Afterwards, a reverse transcriptase PCR was performed by incubating for 90

minutes at 42°C, which is followed by enzymatic inactivation for 20 minutes at 65°C (Figure 10). The cDNA obtained was kept at -20°C.

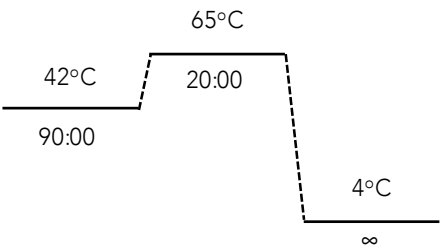


Figure 10. Reverse transcription PCR cycle of cDNA synthesis. cDNA was synthesized for 90 minutes at 42°C and the enzyme was inactivated for 20 minutes at 65°C.

| Real-time Quantitative Polymerase Chain Reaction

For real-time quantitative polymerase chain reaction (RT-qPCR), a mix was prepared containing 2μL of 1:10 diluted synthesized cDNA, 10μL of SyberGreen II Master Mix, 1μL of 1:10 diluted primers (forward and reverse) and 7μL of water making a total of 20μL. A 96 well plate was prepared and a programmed reaction (Figure 11). The fluorescence was measured after the extension step using Applied Biosystems 7500 Real Time PCR System and the corresponding software. After the thermocycling reaction, the melting step was performed with continuous measurement of fluorescence. The analysis was performed using the 2-ΔΔCT method.

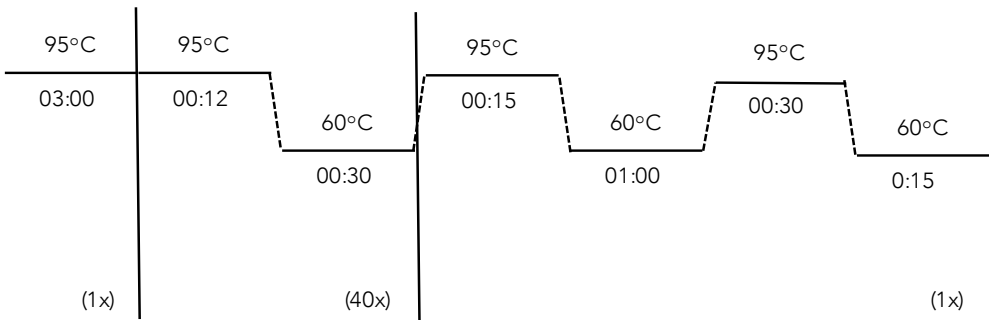


Figure 11. RT-qPCR cycling protocol. The reaction initiated by heating at 95°C for 3 minutes, followed by 40 cycles of 12 seconds denaturation step at 95°C and a 30 seconds annealing/elongation step at 60°C. After thermocycling reaction, the melting step was performed with continuous measurement of fluorescence.

| Protein Extraction and Quantification

| *Lysis protocol*

Cells were washed 3 times with 1x PBS and, after incubating with 125 μ L of Lysis Buffer supplemented with inhibitors per well, they were scraped and transferred for an Eppendorf. To promote disruption of the cell membranes, samples were resuspended 20 times with a syringe of 26G and incubated 30 minutes for 4°C while resuspended every 10 minutes. A centrifugation at 17 000 g for 15 minutes at 4°C allowed the sedimentation of cellular debris being the supernatant transferred to a new tube and kept on ice before proceeding to quantification.

| *Bradford quantification method*

For the Bradford protein assay, 3 μ L of sample were mixed with 97 μ L of 0.1M NaOH in tubes and 1mL of Bradford solution was subsequently added. The samples were next incubated for 15 minutes at room temperature in the dark before optical density measurement at a wavelength of 595nm. Duplicates of each sample were prepared in all experiments. At the same time, a set of standards ranging from 0 to 15 μ g were prepared with bovine serum albumin (BSA) from a stock solution at 1 μ g/ μ L. Each standard tube was filled to a final volume of 100 μ L with the solution of 0.1M NaOH before the addition of 1mL of Bradford solution. The absorbance measured for the standards was used for drawing a standard curve in order to calculate the samples concentration.

| Western Blot

After protein quantification, the samples were prepared for western blot analysis, using 50 μ g of protein.

| *Sodium Dodecyl Sulfate-Polyacrylamide Gel Electrophoresis (SDS-PAGE) and Transfer*

Samples were diluted in 6x Laemmli being afterwards denatured for 5 minutes at 95°C. Subsequently, samples were loaded alongside with a pre-stained protein marker in mini

hand cast gels prepared with 10% polyacrylamide resolving gel and 4% stacking gel. The electrophoretic chamber was filled with 1x Running buffer (25mM Tris, 0.2M Glycine, 20% SDS) and the electrophoresis was conducted for 2 hours, first at 80V to allow the samples to pass through the stacking gel and then at 120V. The bromophenol blue present in the loading buffer allowed sample running visualization.

After protein's separation and migration, proteins were electro-transferred onto a nitrocellulose membrane in the Trans-Blot® SD Semi-Dry Transfer Cell at 25V for 30 minutes.

| *Immunoblotting*

The membranes were washed 3 times, 5 minutes each, with 1x Tris-saline buffer with tween 20 (TBS-T) to take out the methanol residues and then blocked with 5% (w/w) low-fat powder milk diluted in 1x TBS-T for 1 hour at room temperature. Primary antibodies incubation was performed for 1 to 3 hours at room temperature or overnight at 4°C, while the respective secondary antibodies were incubated for 1 hour at room temperature protected from light (if necessary), under agitation. Between blocking and antibodies incubation, membranes were washed 3 times for 5 minutes with 1x TBS-T.

According to the secondary antibody the membranes were analysed by two different methods. Staining of the membrane with fluorescence tagged antibodies allows protein observation in the Odyssey system with the LI-COR software (Biosciences, US). For this fluorescence detection, secondary antibodies are coupled with a fluorescent probe. On the other hand, for chemiluminescence detection, HRP coupled secondary antibodies were used. Clarity western ECL substrate (BioRad) was used to activate HRP and produce luminescent signal. For acquisition and image processing Image Studio Lite or Image Lab Software (BioRad) were used. The quantification of each protein was performed in Image Lab Software (BioRad), using α/β tubulin as a normalizer.

IV. Results and Discussion

Peroxisomes and mitochondria have been shown to act in concert as important signalling platforms within the cellular antiviral response: while the peroxisomal pathway induces a rapid but transient response, the mitochondrial pathway activates a signalling cascade with delayed kinetics that amplifies and stabilizes the antiviral response. Although the mitochondrial signalling pathway is well established, the peroxisomal signalling pathway is still a mystery.

Viruses completely depend on the host cell and, consequently, have evolved mechanisms to evade the antiviral defense, such as avoiding PRR detection or targeting receptors or signalling molecules for degradation to hamper host protein synthesis. In order to unravel the peroxisomal-dependent antiviral signalling pathway we made use of two viral proteins that are known to evade the cellular antiviral defense by hampering the mitochondrial-dependent antiviral response.

4.1 | TRAF3 is involved in the peroxisomal MAVS downstream signalling

Herpes simplex virus 1 (HSV-1) belongs to the *Alphaherpesvirus* subfamily and is a large, linear double-stranded DNA virus. As an extremely successful human pathogen, HSV-1 evolved various mechanisms and immune evasion strategies to overcome the defense of its host^{106,107}.

UL36 is the largest tegument protein of HSV-1 being conserved across the *Herpesviridae* family. It is a multifunctional protein that plays an essential role in the HSV-1 entry, capsid transport and virion assembly, formation of mature virions, microtubule transport of capsids and pathogenesis. UL36 processing produces a 420-amino-acid peptide that exhibits single deubiquitinase (DUB) activity, nominated as UL36 ubiquitin-specific protease (UL36USP)^{108,109}.

Wang *et al.*¹⁰⁹ were the first to demonstrate that ectopic expression of UL36USP was sufficient to downregulate SeV-activated IFN- β promoter activity and that the deubiquitinase activity of UL36USP is necessary for its inhibitory activity. Moreover, these authors also demonstrated that UL36USP cleaved both the K63- and K48-linked polyubiquitin chains of TRAF3, inhibiting the recruitment of TBK1 by TRAF3 and,

consequently the RLR-induced IFN- β production. More recently, Ye *et al.*¹⁰⁸ demonstrated that ectopically expressed UL36USP decreased cGAS-STING-induced IFN- β and NF- κ B promoter activation. It was shown that UL36USP inhibits DNA-induced IFN- β and NF- κ B activation under conditions of HSV-1 infection. Additionally, UL36USP inhibited NF- κ B activation by deubiquitinating I κ B α and restricting its degradation, consequently reducing IFN production¹⁰⁸.

With this, we decided to use UL36-YFP to determine whether TRAF3 is also involved in the peroxisomal MAVS-dependent signalling pathway. To this end, a plasmid encoding UL36-YFP was transfected into MEFs cells that express MAVS solely at peroxisomes (MAVS-PEX cells). Twenty-four hours after transfection, these cells were stimulated for six hours by overexpressing a constitutively active version of RIG-I, which is composed exclusively by the CARD domains of RIG-I (GFP-RIG-I-CARD). GFP-RIG-I-CARD overexpression allows the direct activation of MAVS without needing an activator ligand, therefore mimicking a viral infection^{110,111}.

To confirm UL36-YFP overexpression and localization, cells were observed by confocal microscopy after immunofluorescence analyses with an antibody against the peroxisomal marker PMP70 and DAPI to stain the nucleus. As it is possible to observe in Figure 12, and as Coller *et al.*¹¹² and Abaitua and O'Hare¹¹³ showed in previous works, UL36-YFP overexpression shows cytoplasmic localization with accumulation in perinuclear regions. Furthermore, no co-localization between UL36-YFP and the peroxisomes was observed.

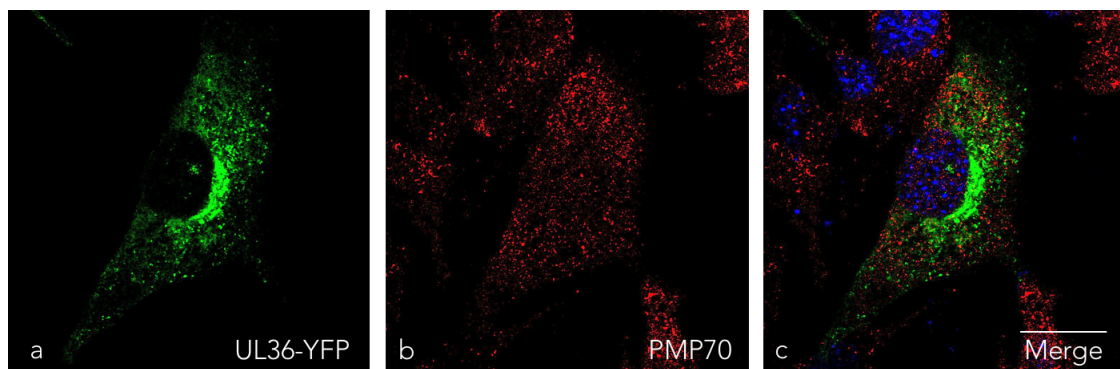


Figure 12. UL36-YFP overexpression in MEFs MAVS-PEX cells. (a) UL36-YFP, (b) PMP70, (c) Merge image of a and b. Bars correspond to 10 μ m.

IRF1 mRNA production was quantified by RT-qPCR and the activation of the signal transducer and activator of transcription 1 (STAT1) was analysed by immunoblotting. IRF1 is one of the ISGs known to be stimulated by the peroxisomal MAVS-dependent signalling pathway and the phosphorylation of the STAT1 corresponds to the activation of the cells by IFN which will consequently induce the production of more ISGs.

Stimulation of cells in the presence of the viral protein UL36-YFP resulted in the inhibition of the IRF1 mRNA production (Figure 13A), as well as in the inhibition of the STAT1 phosphorylation (Figure 13B). Hence, UL36-YFP inhibited the peroxisome-dependent MAVS signalling, strongly suggesting that TRAF3 may be one of the signalling proteins required for activation of this pathway and induction of ISG and IFN production.

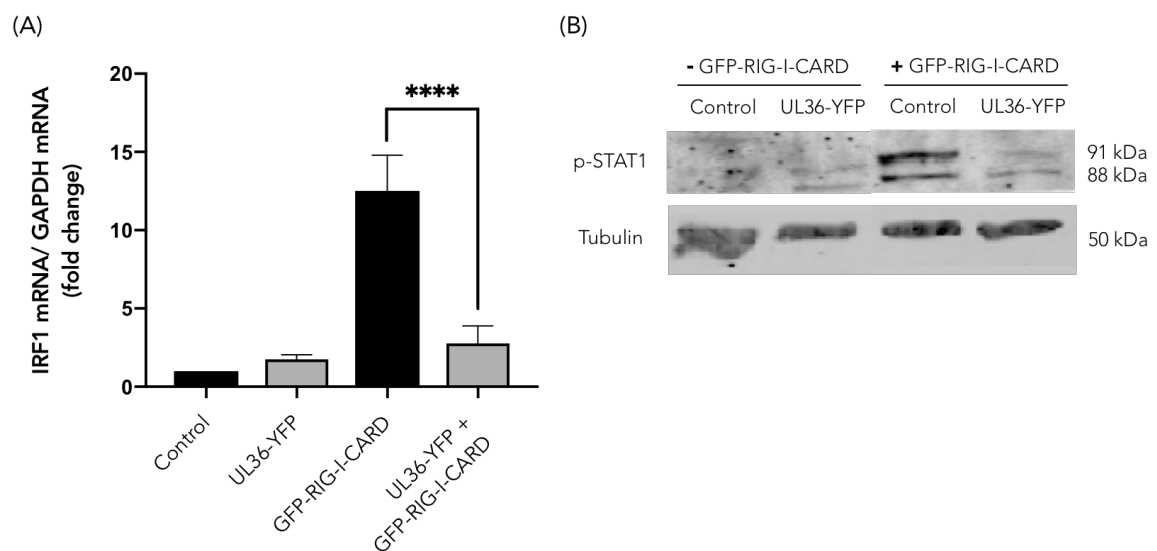


Figure 13. Viral protein UL36-YFP inhibits the peroxisome-dependent innate immunity signalling. MEFs MAVS PEX cells were transfected with viral protein UL36-YFP, and 24 hours later were stimulated with GFP-RIG-I-CARD. (A) Six hours upon stimulation IRF1 mRNA expression was analysed by RT-qPCR. GAPDH was used as a normalizer gene. Data represents the means \pm SEM of 3 independent experiments. Statistical analysis was performed using one-way ANOVA followed by Bonferroni's multiples comparison. Error bars represent SEM. **** $p \leq 0.0001$, compared with control. (B) Phosphorylation of STAT1 was analysed by immunoblotting. Antibodies against p-STAT1 and tubulin were used. Tubulin was used as a loading control.

4.2 | IKK ϵ is involved in the peroxisomal MAVS downstream signalling transduction

Lymphocytic choriomeningitis virus (LCMV), which belongs to the *Arenaviridae* family, is an enveloped virus with a negative-strand RNA genome. LCMV has a non-lytic life cycle usually associated with continued replication and expression of viral proteins in the cytoplasm, being able to escape the innate detection and/or counteract the mechanisms of innate defense^{114,115}.

LCMV NP is the most abundantly produced viral protein and is associated with the viral RNA (vRNA) forming the nucleocapsid. NP is a multifunctional protein with essential roles in host immunosuppression, viral replication and encapsidation of the viral genome¹¹⁶. Martínez-Sobrido *et al.*¹¹⁷ were the first to demonstrate that LCMV NP is able to block the nuclear translocation and transcriptional activity of IRF3, which consequently, results in a significant inhibition of type I IFN production in the host cell. More recently, Pythoud *et al.*¹¹⁵ determined that the LCMV NP specifically targets the IKK ϵ by binding to the kinase domain (KD) of IKK ϵ , blocking its autocatalytic activity and subsequently the phosphorylation of IRF3.

With this, we decided to use HA-NP viral protein as a tool to determine whether IKK ϵ is also involved in the downstream signalling from peroxisomal MAVS. To this end, a plasmid encoding HA-NP was transfected into MAVS-PEX cells, and twenty-four hours after, the cells were stimulated with GFP-RIG-I-CARD to mimic a viral infection, as previously explained.

After confirming the overexpression of HA-NP (Figure 14A), the requirement of IKK ϵ was analysed through quantification of IRF1 mRNA production by RT-qPCR and the activation of STAT1 by immunoblotting.

The results shown in Figure 14B and 14C, indicate that the stimulation of MAVS-PEX cells in the presence of the viral protein HA-NP resulted in the inhibition of the IRF1 mRNA production as well as in the phosphorylation of STAT1.

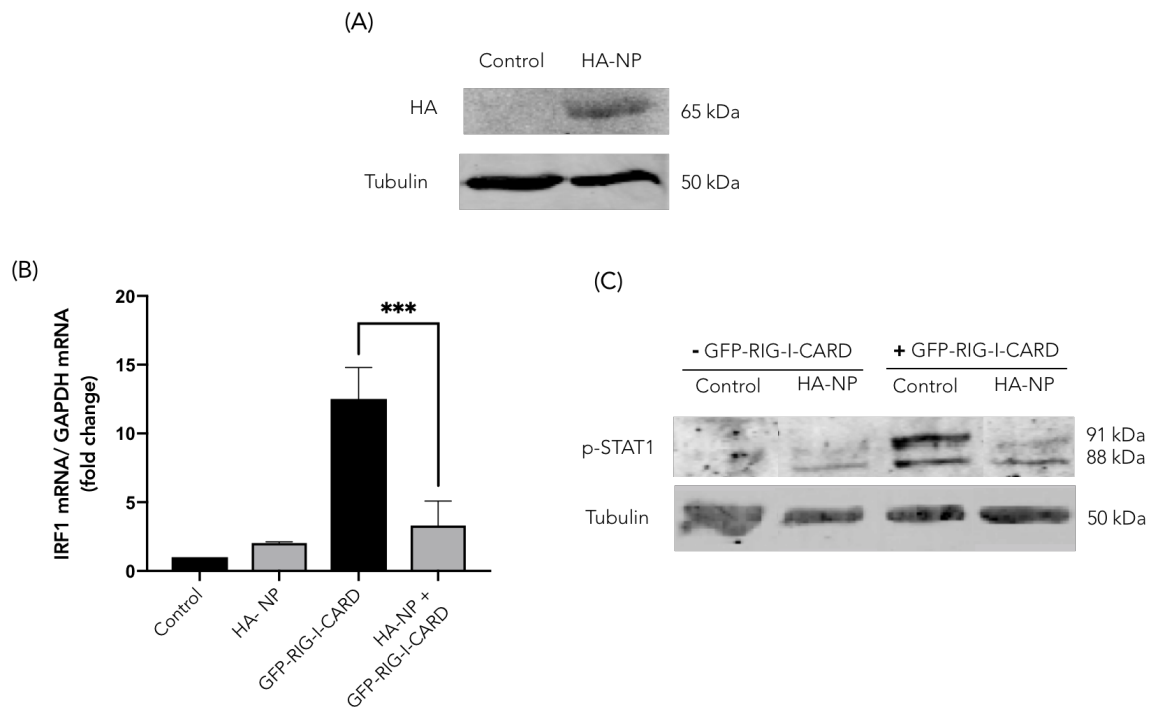


Figure 14. IKK ϵ is involved in the downstream signalling from peroxisomal MAVS. MEFs MAVS PEX cells were transfected with viral protein HA-NP and stimulated with GFP-RIG-I-CARD. (A) IRF1 mRNA expression was analysed by RT-qPCR. GAPDH was used as a normalizer gene. Data represents the means \pm SEM of 3 independent experiments. Statistical analysis was performed using one-way ANOVA followed by Bonferroni's multiples comparison. Error bars represent SEM. *** $p \leq 0.001$, compared with control. (B) Phosphorylation of STAT1 was analysed by immunoblotting. Antibodies against p-STAT1 and tubulin were used. Tubulin was used as a loading control.

IKK ϵ is known to be involved in the mitochondrial MAVS-dependent antiviral signalling pathway. It was described that TRAFs interact with TBK1/IKK ϵ complex upon mitochondrial MAVS activation, which then induces IRF3 phosphorylation and translocation to the nucleus leading to the production of ISG and IFN^{118–120}.

Since in cells that only express MAVS at peroxisomes, overexpression of HA-NP, inhibitor of IKK ϵ , blocked the peroxisomal MAVS downstream signalling, we can predict that IKK ϵ is also involved in the peroxisome-dependent antiviral pathway. Furthermore, and considering that normally IKK ϵ forms a complex with TBK1, we can infer that this complex is required for the peroxisomal-dependent antiviral pathway. Further experiments should be performed to corroborate the requirement of IKK ϵ and TBK1.

Stimulation of cells with an active version of RIG-I can have a secondary effect as this is accomplished by transfecting a dsDNA, which can lead to the activation of the cGAS-STING signalling pathway. In this regard, future experiences are needed where the peroxisomal MAVS-dependent antiviral signalling would be stimulated with poly (I:C), a specific RNA synthetic agonist of RIG-I, assuring that only the RLR pathway is activated.

Up until now, few reports have focused on the role of the peroxisomes in the cellular antiviral defense. Although it is still controversial, it is described that peroxisomal MAVS-dependent pathway culminates in the direct induction of ISGs, and type III IFN in some cells, through the activation of IRF1 complementing the type I IFN production induced by the mitochondrial MAVS downstream pathway^{100,101}. With our results, we disclose new signalling mediators downstream from peroxisomal MAVS, TRAF3 and IKK ϵ . Additionally, these results propose that TBK1 is also involved in the downstream signalling since it interacts with IKK ϵ and is activated by TRAF3. Altogether, our results provide new insights into the peroxisomal MAVS-dependent signalling pathway.

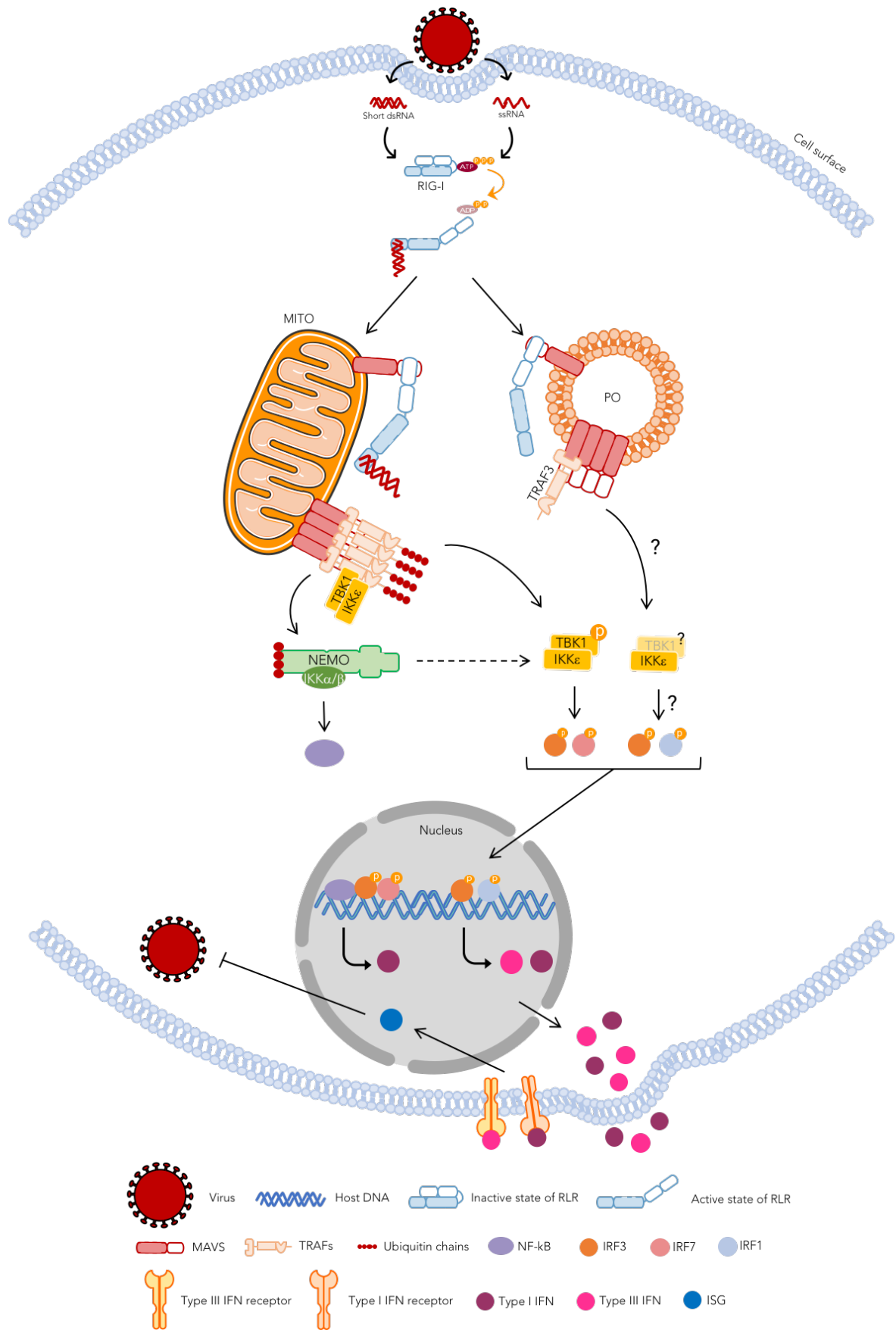


Figure 15. Mitochondrial and peroxisome MAVS-dependent signalling pathway. Once the viral nucleic acid enters the cell, there is an activation of the RIG-I receptor which suffers several conformational changes allowing the MAVS to oligomerize. This oligomerization will induce the activation of multiple downstream molecules that will ultimately lead to the activation of the JAK-STAT pathway. Here we represent what we propose to be the new downstream molecules of the peroxisomal MAVS-dependent signalling pathway. MITO – Mitochondria; PO – Peroxisome.

V. Conclusion

Peroxisomes are dynamic and multifunctional organelles that function as signalling platforms through the cooperation with other organelles. Overtime, more evidences have arisen, demonstrating the importance of peroxisomes not only in physiological processes but also in antiviral immune response.

To guarantee an efficient antiviral response and avoid any dysregulation of the host immune signalling, the antiviral pathway needs to be strongly regulated, being the RLRs the first line of response responsible for the recognition of viral nuclei acid. Upon infection, RIG-I recognizes cytoplasmic viral genome and interact with MAVS both at peroxisomes and mitochondria leading to the activation of several antiviral effectors. Although peroxisomal and mitochondrial MAVS act differently, both have complementing functions, being the peroxisomal MAVS associated to a rapid but short response, while mitochondrial MAVS is responsible for a delayed but long-lasting antiviral response.

Contrary to the mitochondrial MAVS-dependent signalling pathway that is well described and established, the downstream signalling mediators from peroxisomal MAVS remain unknown.

The results obtained with this work have allowed us to unravel some steps of the signalling pathway downstream from peroxisomal MAVS. We suggest that TRAF3 and IKK ϵ are intervenients in the peroxisomal MAVS-dependent signalling pathway, being required for the production of IRF1 and activation of STAT1.

Further experiments should be performed to confirm the results obtained with this study, as well as to unravel other proteins that may interfere with this peroxisomal-dependent antiviral signalling. To this end, we propose using knock-out cells for the identified proteins that express MAVS solely at peroxisomes or perform knock-down experiments in MAVS-PEX cells. Additionally, other viral proteins that restrict other antiviral signalling proteins could be overexpressed to identify new mediators of the peroxisomal MAVS-dependent antiviral pathway.

VI. References

1. Rhodin J. Electron on Renal Physiology Microscopy of the Kidney. *Symp Ren Physiol*. 1958.
2. De Duve C, Baudhuin P. Peroxisomes (Microbodies and Related Particles).pdf. *Physiol Rev*. 1966;46(2):323-352.
3. Schrader M, Fahimi HD. The peroxisome: Still a mysterious organelle. *Histochem Cell Biol*. 2008;129:421-440. doi:10.1007/s00418-008-0396-9.
4. Islinger M, Schrader M. Peroxisomes. *Curr Biol*. 2011;21(19):R800-R801. doi:10.1016/j.cub.2011.07.024.
5. Ribeiro D, Castro I, Dariush Fahimi H, Schrader M. Peroxisome morphology in pathology. *Histol Histopathol*. 2012;27(6):661-676.
6. Gabaldón T. Peroxisome diversity and evolution. *Philos Trans R Soc B Biol Sci*. 2010;365:765-773. doi:10.1098/rstb.2009.0240.
7. Heiland I, Erdmann R. Biogenesis of peroxisomes. Topogenesis of the peroxisomal membrane and matrix proteins. *FEBS J*. 2005;272:2362-2372. doi:10.1111/j.1742-4658.2005.04690.x.
8. Odendall C, Kagan JC. Peroxisomes and the Antiviral Responses of Mammalian Cells. *Subcell Biochem*. 2013;69:67-75. doi:10.1007/978-94-007-6889-5.
9. Cipolla CM, Lodhi IJ. Cipolla and Lodhi, 2017.pdf. *Trends Endocrinol Metab*. 2017;28(4):297-308.
10. Dahabieh MS, Di Pietro E, Jangal M, et al. Peroxisomes and cancer: The role of a metabolic specialist in a disease of aberrant metabolism. *Biochim Biophys Acta - Rev Cancer*. 2018;1870:103-121. doi:10.1016/j.bbcan.2018.07.004.
11. Ma C, Agrawal G, Subramani S. Peroxisome assembly: Matrix and membrane protein biogenesis. *J Cell Biol*. 2011;193(1):7-16. doi:10.1083/jcb.201010022.
12. Hettema EH, Motley AM. How peroxisomes multiply. 2009. doi:10.1242/jcs.034363.
13. Costello JL, Castro IG, Hacker C, et al. ACBD5 and VAPB mediate membrane associations between peroxisomes and the ER. 2017;216(2):331-342.
14. Hettema EH, Motley AM. How peroxisomes multiply. *J Cell Sci*. 2009;122(14):2331-2336. doi:10.1242/jcs.034363.

15. Farré J, Mahalingam SS, Proietto M, Subramani S. Peroxisome biogenesis, membrane contact sites, and quality control. *EMBO Rep.* 2018;20(1):e46864. doi:10.15252/embr.201846864.
16. Lazarow PB. Peroxisome biogenesis: Advances and conundrums. *Curr Opin Cell Biol.* 2003;15:489-497. doi:10.1016/S0955-0674(03)00082-6.
17. Tabak HF, van der Zand A, Braakman I. Peroxisomes: minted by the ER. *Curr Opin Cell Biol.* 2008;20:393-400. doi:10.1016/j.ceb.2008.05.008.
18. Farré J, Mahalingam SS, Proietto M, Subramani S. Peroxisome biogenesis, membrane contact sites, and quality control. *EMBO Rep.* 2018;20(1):e46864. doi:10.15252/embr.201846864.
19. Fujiki Y, Matsuzono Y, Matsuzaki T, Fransen M. Import of peroxisomal membrane proteins: The interplay of Pex3p- and Pex19p-mediated interactions. *Biochim Biophys Acta - Mol Cell Res.* 2006;1763:1639-1646. doi:10.1016/j.bbamcr.2006.09.030.
20. Schrader M, Fahimi HD. Growth and Division of Peroxisomes. *Int Rev Cytol.* 2006;255:237-290. doi:10.1016/S0074-7696(06)55005-3.
21. Lazarow PB, Fujiki Y. Biogenesis of Peroxisomes. *Annu Rev Cell Dev Biol.* 1985;1:489-530.
22. Brown L-A, Baker A. Shuttles and cycles: transport of proteins into the peroxisome matrix.pdf. 2008:363-375.
23. Hasan S, Platta HW, Erdmann R. Import of proteins into the peroxisomal matrix. *Front Physiol.* 2013;4:1-12. doi:10.3389/fphys.2013.00261.
24. Castro IG, Richards DM, Passmore JB, et al. A role for Mitochondrial Rho GTPase 1 (MIRO1) in motility and membrane dynamics of peroxisomes. *Wiley Traffic.* 2018;19:229-242. doi:10.1111/tra.12549.
25. Opaliński Ł, Kiel JAKW, Williams C, Veenhuis M, Van Der Klei IJ. Membrane curvature during peroxisome fission requires Pex11. *EMBO J.* 2011;30:5-16. doi:10.1038/emboj.2010.299.
26. Koch J, Brocard C. PEX11 proteins attract Mff and human Fis1 to coordinate peroxisomal fission. *J Cell Sci.* 2012;125(16):3813-3826. doi:10.1242/jcs.102178.

27. Li X, Gould SJ. MEMBRANE TRANSPORT STRUCTURE FUNCTION AND BIOGENESIS : The Dynamin-like GTPase DLP1 Is Essential for Peroxisome Division and Is Recruited to Peroxisomes in Part by PEX11 The Dynamin-like GTPase DLP1 Is Essential for Peroxisome Division and Is Recruited to. *J Biol Chem*. 2003;278(19):17012-17020. doi:10.1074/jbc.M212031200.
28. Schrader M, Reuber BE, Morrell JC, et al. Expression of PEX11 β Mediates Peroxisome Proliferation in the Absence of Extracellular Stimuli. *J Biol Chem*. 2002;273(45):29607-29614. doi:10.1074/jbc.273.45.29607.
29. Hoepfner D, Schildknecht D, Braakman I, Philippsen P, Tabak HF. Contribution of the endoplasmic reticulum to peroxisome formation. *Cell*. 2005;122(1):85-95. doi:10.1016/j.cell.2005.04.025.
30. Agrawal G, Subramani S. De novo peroxisome biogenesis: evolving concepts and conundrums. 2016;25(3):289-313. doi:10.1007/s11065-015-9294-9.Functional.
31. Agrawal G, Fassas SN, Xia ZJ, Subramani S. Distinct requirements for intra-ER sorting and budding of peroxisomal membrane proteins from the ER. *J Cell Biol*. 2016;212(3):335-348. doi:10.1083/jcb.201506141.
32. Wanders RJA. Metabolic functions of peroxisomes in health and disease. *Biochimie*. 2014;98:36-44. doi:10.1016/j.biochi.2013.08.022.
33. Lazarow PB. The role of peroxisomes in mammalian cellular metabolism. *J Inherit Metab Dis*. 1987;10(1 Supplement):11-22. doi:10.1007/BF01812843.
34. Fransen M, Nordgren M, Wang B, Apanasets O. Role of peroxisomes in ROS/RNS-metabolism: Implications for human disease. *Biochim Biophys Acta - Mol Basis Dis*. 2012;1822(9):1363-1373. doi:10.1016/j.bbadis.2011.12.001.
35. Waterham HR, Ferdinandusse S, Wanders RJA. Human disorders of peroxisome metabolism and biogenesis. *Biochim Biophys Acta - Mol Cell Res*. 2016;1863:922-933. doi:10.1016/j.bbamcr.2015.11.015.
36. Chance B, Sies H, Boveris A. Hydroperoxide metabolism in mammalian organs. *Physiol Rev*. 1979;59(3):527-605. doi:10.1152/physrev.1979.59.3.527.
37. Braverman NE, Moser AB. Functions of plasmalogen lipids in health and disease. *Biochim Biophys Acta - Mol Basis Dis*. 2012;1822(9):1442-1452.

- doi:10.1016/j.bbadis.2012.05.008.
38. Wanders RJA, Waterham HR. Biochemistry of Mammalian Peroxisomes Revisited. *Annu Rev Biochem.* 2006;75:295-332.
 39. Schrader M, Godinho LF, Costello JL, Islinger M. The different facets of organelle interplay—an overview of organelle interactions. *Front Cell Dev Biol.* 2015;3(September):1-22. doi:10.3389/fcell.2015.00056.
 40. Schrader M, Grille S, Fahimi HD, Islinger M. Peroxisomes Interactions and Cross-Talk with Other Subcellular Compartments in Animal Cells. *Subcell Biochem.* 2013;69:117-120. doi:10.1007/978-94-007-6889-5.
 41. Demarquoy J, Borgne F Le. Crosstalk between mitochondria and peroxisomes. *World J Biol Chem.* 2015;6(4):301-309. doi:10.4331/wjbc.v6.i4.301.
 42. Schrader M, Costello J, Godinho LF, Islinger M. Peroxisome-mitochondria interplay and disease. *J Inherit Metab Dis.* 2015. doi:10.1007/s10545-015-9819-7.
 43. Fransen M, Lismont C, Walton P. The Peroxisome-Mitochondria Connection: How and Why? *Int J Mol Sci.* 2017;18.
 44. Schrader M, Yoon Y. Mitochondria and peroxisomes: Are the “Big Brother” and the “Little Sister” closer than assumed? *BioEssays.* 2007;29(11):1105-1114. doi:10.1002/bies.20659.
 45. Thoms S, Grønborg S, Gärtner J. Organelle interplay in peroxisomal disorders. *Trends Mol Med.* 2009;15(7):293-302. doi:10.1016/j.molmed.2009.05.002.
 46. Schuldiner M, Zalckvar E. Incredibly close-A newly identified peroxisome-ER contact site in humans. *J Cell Biol.* 2017;216(2):287-289. doi:10.1083/jcb.201701072.
 47. Chu BB, Liao YC, Qi W, et al. Cholesterol transport through lysosome-peroxisome membrane contacts. *Cell.* 2015;161:291-306. doi:10.1016/j.cell.2015.02.019.
 48. Jin Y, Strunk BS, Weisman LS. Close encounters of the lysosome/peroxisome kind. *Cell.* 2015;161(2):197-198. doi:10.1177/0333102415576222.Is.
 49. Binns D, Januszewski T, Chen Y, et al. An intimate collaboration between peroxisomes and lipid bodies. *J Cell Biol.* 2006;173(5):719-731. doi:10.1083/jcb.200511125.
 50. Guimaraes SC, Schuster M, Bielska E, et al. Peroxisomes, lipid droplets, and

- endoplasmic reticulum “hitchhike” on motile early endosomes. *J Cell Biol.* 2015;211(5):945-954. doi:10.1083/jcb.201505086.
51. Schrader M. Tubulo-Reticular Clusters of Peroxisomes in Living COS-7 Cells: Dynamic Behavior and Association with Lipid Droplets.pdf. *J Histochem Cytochem.* 2001;49(11):1421-1429.
 52. Kohlwein SD, Veenhuis M, van der Klei IJ. Lipid droplets and peroxisomes: Key players in cellular lipid homeostasis or a matter of fat-store’em up or burn’em down. *Genetics.* 2013;193:1-50. doi:10.1534/genetics.112.143362.
 53. Janeway CA. Approaching the asymptote. Evolution and revolution in immunity. *Cold Spring Harb Symp Quant Biol.* 1989;54:1-13. doi:10.1101/SQB.1989.054.01.003.
 54. Mogensen TH. Pathogen recognition and inflammatory signaling in innate immune defenses. *Clin Microbiol Rev.* 2009;22(2):240-273. doi:10.1128/CMR.00046-08.
 55. Mogensen TH. Pathogen recognition and inflammatory signaling in innate immune defenses. *Clin Microbiol Rev.* 2009;22(2):240-273. doi:10.1128/CMR.00046-08.
 56. Jiang X, Kinch L, Brautigam CA, et al. NIH Public Access. *Immunity.* 2012;36(6):959-973. doi:10.1016/j.immuni.2012.03.022.Ubiquitin-Induced.
 57. Wilkins C, Jr MG. Recognition of viruses by cytoplasmic sensors. *Curr Opin Immunol.* 2010;22(1):41-47. doi:10.1016/j.coi.2009.12.003.Recognition.
 58. Liu Y, Olganier D, Lin R. Host and Viral Modulation of RIG-I-Mediated Antiviral Immunity. *Front Immunol.* 2017;7:662.
 59. Chow J, Franz KM, Kagan JC. PRRs are watching you: Localization of innate sensing and signalling regulators. *Virology.* 2015;479-480:104-109. doi:10.1177/0333102415576222.Is.
 60. Chuenchor W, Jin T, Ravilious G, Xiao TS. Structures of pattern recognition receptors reveal molecular mechanisms of autoinhibition, ligand recognition and oligomerization. *Curr Opin Immunol.* 2014;26:14-20. doi:10.1158/0008-5472.CAN-10-4002.BONE.
 61. Kawai T, Akira S. The role of pattern-recognition receptors in innate immunity: Update on toll-like receptors. *Nat Immunol.* 2010;11(5):373-384.

- doi:10.1038/ni.1863.
62. Kawai T, Akira S. Toll-like Receptors and Their Crosstalk with Other Innate Receptors in Infection and Immunity. *Immunity*. 2011;34(5):637-650. doi:10.1016/j.immuni.2011.05.006.
 63. Suresh R, Mosser DM. Pattern recognition receptors in innate immunity, host defense, and immunopathology. *Adv Physiol Educ*. 2013;37:284-291. doi:10.1152/advan.00058.2013.
 64. Thompson MR, Kaminski JJ, Kurt-Jones EA, Fitzgerald KA. Pattern recognition receptors and the innate immune response to viral infection. *Viruses*. 2011;3:920-940. doi:10.3390/v3060920.
 65. Lim K-H, Staudt LM. Toll-like Receptor Signaling. *Cold Spring Harb Perspect Biol*. 2013;5(1):a011247. doi:10.1074/jbc.R300028200.
 66. Thompson MR, Kaminski JJ, Kurt-Jones EA, Fitzgerald KA. Pattern recognition receptors and the innate immune response to viral infection. *Viruses*. 2011;3(6):920-940. doi:10.3390/v3060920.
 67. Kumar H, Kawai T, Akira S. Pathogen recognition by the innate immune system. *Int Rev Immunol*. 2011;30:16-34. doi:10.3109/08830185.2010.529976.
 68. Sun L, Wu J, Du F, Chen X, Chen ZJ. Cyclic GMP-AMP Synthase is a Cytosolic DNA Sensor that Activates the Type-I Interferon Pathway. *Science (80-)*. 2013;339(6121). doi:10.1016/j.pestbp.2011.02.012.Investigations.
 69. Cai X, Chiu YH, Chen ZJ. The cGAS-cGAMP-STING pathway of cytosolic DNA sensing and signaling. *Mol Cell*. 2014;54:289-296. doi:10.1016/j.molcel.2014.03.040.
 70. Rathinam VA, Fitzgerald KA. Cytosolic surveillance and antiviral immunity. *Curr Opin Virol*. 2011;1(6):455-462. doi:10.1161/ATVBAHA.114.303112.ApoA-I.
 71. Ori D, Murase M, Kawai T. Cytosolic nucleic acid sensors and innate immune regulation. *Int Rev Immunol*. 2017.
 72. Chen Q, Sun L, Chen ZJ. Regulation and function of the cGAS-STING pathway of cytosolic DNA sensing. *Nat Immunol*. 2016;17(10):1142-1149.
 73. Jiang X, Kinch L, Brautigam CA, et al. Ubiquitin-Induced Oligomerization of the RNA Sensors RIG-I and MDA5 Activates Antiviral Innate Immune Response.

- Immunity*. 2012;36(6):959-973. doi:10.1158/0008-5472.CAN-10-4002.BONE.
74. Loo Y-M, Gale M. Immune signaling by RIG-I-like receptors. *Immunity*. 2011;34(5):680-692. doi:10.1016/j.immuni.2011.05.003.Immune.
75. Bruns A, Horvath CM. Activation of RIG-I-like Receptor Signal Transduction. *Crit Rev Biochem Mol Biol*. 2012;47(2):194-206. doi:10.1161/ATVBAHA.114.303112.ApoA-I.
76. Reikine S, Nguyen JB, Modis Y. Pattern recognition and signaling mechanisms of RIG-I and MDA5. *Front Immunol*. 2014;5:342. doi:10.3389/fimmu.2014.00342.
77. Kolakofsky D, Kowalinski EVA, Cusack S. A structure-based model of RIG-I activation. 2012;18:2118-2127. doi:10.1261/rna.035949.112.2118.
78. Kowalinski E, Lunardi T, McCarthy AA, et al. Structural Basis for the Activation of Innate Immune Pattern-Recognition Receptor RIG-I by Viral RNA. *Cell*. 2011;147:423-435. doi:10.1016/j.cell.2011.09.039.
79. Ramanathan A, Devarkar SC, Jiang F, et al. The autoinhibitory CARD2-Hel2i Interface of RIG-I governs RNA selection. *Nucleic Acids Res*. 2016;44(2):896-909. doi:10.1093/nar/gkv1299.
80. Hou F, Sun L, Zheng H, Skaug B, Jiang Q-X, Chen ZJ. MAVS Forms Functional Prion-Like Aggregates To Activate and Propagate Antiviral Innate Immune Response. *Cell*. 2011;146(3):448-461. doi:10.1002/hbm.21045.Effects.
81. Meylan E, Curran J, Hofmann K, Moradpour D, Binder M, Bartenschlager R. Cardif is an adaptor protein in the RIG-I antiviral pathway and is targeted by hepatitis C virus. 2005;437(October):1167-1172. doi:10.1038/nature04193.
82. Gack MU, Shin YC, Joo C, et al. TRIM25 RING-finger E3 ubiquitin ligase is essential for RIG-I-mediated antiviral activity. *Nature*. 2007;446:916-921. doi:10.1038/nature05732.
83. Chow J, Franz KM, Kagan JC. PRRs are watching you: Localization of innate sensing and signaling regulators. *Virology*. 2015;0:104-109. doi:10.1007/s11065-015-9294-9.Functional.
84. Seth RB, Sun L, Ea CK, Chen ZJ. Identification and characterization of MAVS, a mitochondrial antiviral signaling protein that activates NF- κ B and IRF3. *Cell*.

- 2005;122:669-682. doi:10.1016/j.cell.2005.08.012.
85. Kawai T, Takahashi K, Sato S, et al. Mda5-mediated type I interferon induction. 2005;6(10):981-988. doi:10.1038/ni1243.
 86. Xu L, Wang Y, Han K, et al. VISA Is an Adapter Protein Required for Virus-Triggered IFN- α Signaling. 2005;19:727-740. doi:10.1016/j.molcel.2005.08.014.
 87. Kumar H, Kawai T, Kato H, et al. Essential role of IPS-1 in innate immune responses against RNA viruses. *J Exp Med*. 2006;203(7):1795-1803. doi:10.1084/jem.20060792.
 88. Xu H, He X, Zheng H, et al. Structural basis for the prion-like MAVS filaments in antiviral innate immunity. *Elife*. 2014;3:e01489:1-25. doi:10.7554/elife.01489.
 89. Baril M, Racine M-E, Penin F, Lamarre D. MAVS Dimer Is a Crucial Signaling Component of Innate Immunity and the Target of Hepatitis C Virus NS3/4A Protease. *J Virol*. 2008;83(3):1299-1311. doi:10.1128/jvi.01659-08.
 90. Belgnaoui SM, Paz S, Hiscott J. Orchestrating the interferon antiviral response through the mitochondrial antiviral signaling (MAVS) adapter. *Curr Opin Immunol*. 2011;23(5):564-572. doi:10.1016/j.coi.2011.08.001.
 91. Bender S, Reuter A, Eberle F, Einhorn E, Binder M. Activation of Type I and III Interferon Response by Mitochondrial and Peroxisomal MAVS and Inhibition by Hepatitis C Virus. 2015:1-30. doi:10.1371/journal.ppat.1005264.
 92. Liu S, Chen J, Cai X, et al. MAVS recruits multiple ubiquitin E3 ligases to activate antiviral signaling cascades. 2013;2:e00785:1-24. doi:10.7554/eLife.00785.
 93. Oganessian G, Saha SK, Guo B, et al. Critical role of TRAF3 in the Toll-like receptor-dependent and -independent antiviral response. 2006;439(January):10-13. doi:10.1038/nature04374.
 94. Fang R, Jiang Q, Zhou X, et al. MAVS activates TBK1 and IKK ϵ through TRAFs in NEMO dependent and independent manner. *PLoS Pathog*. 2017;13(11):1-22. doi:10.1371/journal.ppat.1006720.
 95. Saha SK, Pietras EM, He JQ, et al. Regulation of antiviral responses by a direct and specific interaction between TRAF3 and Cardif. 2006;25(14):3257-3263. doi:10.1038/sj.emboj.7601220.
 96. Hayden MS, Ghosh S. Signaling to NF- κ B. *Genes Dev*. 2004;18:2195-2224.

- doi:10.1101/gad.1228704.bone.
97. Tokunaga F, Sakata SI, Saeki Y, et al. Involvement of linear polyubiquitylation of NEMO in NF- κ B activation. *Nat Cell Biol.* 2009;11(2):123-132. doi:10.1038/ncb1821.
 98. Belgnaoui SM, Paz S, Samuel S, et al. Linear ubiquitination of NEMO negatively regulates the interferon antiviral response through disruption of the MAVS-TRAF3 complex. *Cell Host Microbe.* 2012;12:211-222. doi:10.1016/j.chom.2012.06.009.
 99. Karin M, Ben-Neriah Y. Phosphorylation Meets Ubiquitination: The Control of NF- κ B Activity. *Annu Rev Immunol.* 2000;18:621-663.
 100. Dixit E, Boulant S, Zhang Y, et al. Peroxisomes are signaling platforms for antiviral innate immunity. *Cell.* 2010;141(4):668-681.
doi:10.1016/j.cell.2010.04.018.Peroxisomes.
 101. Odendall C, Dixit E, Stavru F, et al. Diverse intracellular pathogens activate Type III Interferon expression from peroxisomes. *Nat Commun.* 2014;15(8):717-726.
doi:10.1002/jmri.25711.PET/MRI.
 102. Kagan JC. Signaling organelles of the innate immune system. *Cell.* 2012;151:1168-1178. doi:10.1016/j.cell.2012.11.011.
 103. Sharma S, Fitzgerald KA. Viral Defense: It Takes Two MAVS to Tango. *Cell.* 2010;141:570-572. doi:10.1016/j.cell.2010.04.043.
 104. Ding S, Robek MD. Peroxisomal MAVS activates IRF1-mediated IFN- γ production. *Nat Immunol.* 2014;15(8):700-701.
 105. Magalhães AC, Ferreira AR, Gomes S, et al. Peroxisomes are platforms for cytomegalovirus' evasion from the cellular immune response. *Sci Rep.* 2016;6:1-14.
doi:10.1038/srep26028.
 106. Arduino PG, Porter SR. Herpes Simplex Virus Type 1 infection: Overview on relevant clinico-pathological features. *J Oral Pathol Med.* 2008;37:107-121.
doi:10.1111/j.1600-0714.2007.00586.x.
 107. Whitley RJ, Roizman B. Herpes Simplex Virus Infections. *Lancet.* 2001;357:1513-1518. <https://www.clinicalkey.es/#!/content/book/3-s2.0-B9781455750177003743>.
 108. Ye R, Su C, Xu H, Zheng C. Specific Protease UL36 Abrogates NF- κ B Activation in DNA Sensing Signal. *J Virol.* 2017;91(5):1-10. doi:10.1038/nmat5031.

109. Wang S, Wang K, Li J, Zheng C. Herpes Simplex Virus 1 Ubiquitin-Specific Protease UL36 Inhibits Beta Interferon Production by Deubiquitinating TRAF3. *J Virol.* 2013;87(21):11851-11860. doi:10.1128/jvi.01211-13.
110. Magalhães AC, Ferreira AR, Gomes S, et al. Peroxisomes are platforms for cytomegalovirus ' evasion from the cellular immune response. *Nat Publ Gr.* 2016;(September 2015):1-14. doi:10.1038/srep26028.
111. Ferreira AR, Magalh AC, Kagan JC, Ribeiro D. Hepatitis C virus NS3-4A inhibits the peroxisomal MAVS-dependent antiviral signalling response. 2016;20(4):750-757. doi:10.1111/jcmm.12801.
112. Collier KE, Lee JI-H, Ueda A, Smith GA. The Capsid and Tegument of the Alphaherpesviruses Are Linked by an Interaction between the UL25 and VP1/2 Proteins. *J Virol.* 2007;81(21):11790-11797. doi:10.1128/jvi.01113-07.
113. Abaitua F, O'Hare P. Identification of a Highly Conserved, Functional Nuclear Localization Signal within the N-Terminal Region of Herpes Simplex Virus Type 1 VP1-2 Tegument Protein. *J Virol.* 2008;82(11):5234-5244. doi:10.1128/jvi.02497-07.
114. Lee KJ, Novella IS, Teng MN, Oldstone MB, de La Torre JC. NP and L proteins of lymphocytic choriomeningitis virus (LCMV) are sufficient for efficient transcription and replication of LCMV genomic RNA analogs. *J Virol.* 2000;74(8):3470-3477. <http://www.ncbi.nlm.nih.gov/pubmed/10729120><http://www.pubmedcentral.nih.gov/articlerender.fcgi?artid=PMC111854>.
115. Pythoud C, Rodrigo WWSI, Pasqual G, Rothenberger S, Martínez-sobrido L. Arenavirus Nucleoprotein Targets Interferon Regulatory Factor-Activating Kinase IKK. 2012;86(15):7728-7738. doi:10.1128/JVI.00187-12.
116. West BR, Hastie KM, Saphire EO. Structure of the LCMV nucleoprotein provides a template for understanding arenavirus replication and immunosuppression. *Acta Crystallogr Sect D Biol Crystallogr.* 2014;70:1764-1769. doi:10.1107/S1399004714007883.
117. Martinez-Sobrido L, Zuniga EI, Rosario D, Garcia-Sastre A, de la Torre JC. Inhibition of the Type I Interferon Response by the Nucleoprotein of the Prototypic Arenavirus Lymphocytic Choriomeningitis Virus. *J Virol.* 2006;80(18):9192-9199.

doi:10.1128/jvi.00555-06.

118. Sonia S, Benjamin R. T, Nathalie G, Guo-Ping Z, Rongtuan L, John H. Triggering the interferon antiviral response through an IKK-related pathway. *Science* (80-). 2003;300:1148-1151.
119. Fitzgerald KA, McWhirter SM, Faia KL, et al. IKKE and TBK1 are essential components of the IRF3 signalling pathway. *Nat Immunol.* 2003;4(5):491-496. doi:10.1038/ni921.
120. Mcwhirter SM, Fitzgerald KA, Rosains J, Rowe DC, Golenbock DT, Maniatis T. IFN-regulatory factor 3-dependent gene expression is defective in Tbk1-deficient mouse embryonic fibroblasts. 2003.